Disorder is a critical component of lipoprotein sorting in Gram-negative bacteria

Jessica El Rayes, Joanna Szewczyk, Michaël Deghelt, Naemi Csoma, André Matagne, Bogdan Iorga, Seung-Hyun Cho, Jean-François Collet

Disorder is a critical component of lipoprotein sorting in Gram-negative bacteria

Jessica El Rayes[1,2$], Joanna Szewczyk[1,2$], Michael Deghelt[1,2], Naemi Csoma[1,2], André Matagne[3], Bogdan I. Iorga[4], Seung-Hyun Cho[1,2], and Jean-François Collet[1,2*]

[1]WELBIO, Avenue Hippocrate 75, 1200 Brussels, Belgium.

[2]de Duve Institute, Université catholique de Louvain, Avenue Hippocrate 75, 1200 Brussels, Belgium.

[3]Centre d'ingéniérie des Protéines, Institut de Chimie B6, Université de Liège, Allée de la Chimie 3, 4000 Liège, Sart Tilman, Belgium.

[4]Université Paris-Saclay, CNRS UPR 2301, Institut de Chimie des Substances Naturelles, 91198 Gif-sur-Yvette, France.

[$]Both authors contributed equally to the work

*Correspondence: jfcollet@uclouvain.be

Abstract (150 max)

Gram-negative bacteria express structurally diverse lipoproteins in their envelope. Here we found that approximately half of lipoproteins destined to the *Escherichia coli* outer membrane display an intrinsically disordered linker at their N-terminus. Intrinsically disordered regions are common in proteins, but establishing their importance *in vivo* has remained challenging. As we sought to unravel how lipoproteins mature, we discovered that unstructured linkers are required for optimal trafficking by the Lol lipoprotein sorting system: linker deletion re-routes three unrelated lipoproteins to the inner membrane. Focusing on the stress sensor RcsF, we found that replacing the linker with an artificial peptide restored normal outer membrane targeting only when the peptide was of similar length and disordered. Overall, this study reveals the role played by intrinsic disorder in lipoprotein sorting, providing mechanistic insight into the biogenesis of these proteins and suggesting that evolution can select for intrinsic disorder that supports protein function.

Introduction

The cell envelope is the morphological hallmark of *Escherichia coli* and other Gram-negative bacteria. It is composed of the inner membrane, a classical phospholipid bilayer, as well as the outer membrane, an asymmetric bilayer with phospholipids in the inner leaflet and lipopolysaccharides in the outer leaflet[1]. This lipid asymmetry enables the outer membrane to function as a barrier that effectively prevents the diffusion of toxic compounds in the environment into the cell. The inner and outer membranes are separated by the periplasm, a viscous compartment that contains a thin layer of peptidoglycan also known as the cell wall[1]. The cell envelope is essential for growth and survival, as illustrated by the fact that several antibiotics such as the β-lactams target mechanisms of envelope assembly. Mechanisms involved in envelope biogenesis and maintenance are therefore attractive targets for novel antibacterial strategies.

Approximately one-third of *E. coli* proteins are targeted to the envelope, either as soluble proteins present in the periplasm or as proteins inserted in one of the two membranes[2]. While inner membrane proteins cross the lipid bilayer via one or more hydrophobic α-helices, proteins inserted in the outer membrane generally adopt a β-barrel conformation[3]. Another important group of envelope proteins is the lipoproteins, which are globular proteins anchored to one of the two membranes by a lipid moiety[4]. Lipoproteins carry out a variety of important functions in the cell envelope: they participate in the biogenesis of the outer membrane by inserting lipopolysaccharide molecules[5,6] and β-barrel proteins[7], they function as stress sensors triggering signal transduction cascades when envelope integrity is altered[8], and they control processes that are important for virulence[9]. The diverse roles played by lipoproteins in the cell envelope has drawn a lot of attention lately, revealing how crucial these proteins are in a wide range of vital processes and identifying them as attractive targets for antibiotic development.

Yet, a detailed understanding of the mechanisms involved in lipoprotein maturation and trafficking is still missing.

Lipoproteins are synthesized in the cytoplasm as precursors with an N-terminal signal peptide[10]. The last four C-terminal residues of this signal peptide, known as the lipobox, function as a molecular determinant of lipid modification unique to bacteria; only the cysteine at the last position of the lipobox is strictly conserved[11]. After translocation across the inner membrane, processing of pre-prolipoproteins into mature forms takes place on the periplasmic side of the membrane. The thiol side-chain of the cysteine is first modified with a diacylglyceryl moiety by prolipoprotein diacylglyceryl transferase (Lgt)[10] (**Supplementary Data Fig. 1a**, step 1). Then, signal peptidase II (LspA) catalyzes cleavage of the signal peptide N-terminally of the lipidated cysteine before apolipoprotein N-acyltransferase (Lnt) adds a third acyl group to the N-terminal amino group of the cysteine (**Supplementary Data Fig. 1a**, steps 2-3). Most mature lipoproteins are then transported to the outer membrane by the Lol system. Lol consists of LolCDE, an ABC transporter that extracts lipoproteins from the inner membrane and transfers them to the soluble periplasmic chaperone LolA (**Supplementary Data Fig. 1a**, steps 4-5)[12]. LolA escorts lipoproteins across the periplasm, binding their hydrophobic lipid tail, and delivers them to the outer membrane lipoprotein LolB (**Supplementary Data Fig. 1a**, step 6). LolB finally anchors lipoproteins to the inner leaflet of the outer membrane using a mechanism that remains poorly characterized (**Supplementary Data Fig. 1a**, step 7).

In most Gram-negative bacteria, a few lipoproteins remain in the inner membrane[13]. The current view is that inner membrane retention depends on the identity of the two residues located immediately downstream of the N-terminal cysteine on which the lipid moiety is

attached[14]; this sequence, two amino acids in length, is known as the Lol sorting signal. When lipoproteins have an aspartate at position +2 and an aspartate, glutamate, or glutamine at position +3, they remain in the inner membrane[15,16], possibly because strong electrostatic interactions between the +2 aspartate and membrane phospholipids prevent their interaction with LolCDE[17]. However, this model is largely based on data obtained in *E. coli* and variations have been described in other bacteria. For instance, in the pathogen *Pseudomonas aeruginosa*, an aspartate is rarely found at position +2 and inner membrane retention appears to be determined by residues +3 and +4[18,19]. Surprisingly, lipoproteins are well sorted in *P. aeruginosa* cells expressing the *E. coli* LolCDE complex[20], despite their different Lol sorting signal. This result cannot be explained by the current model of lipoprotein sorting, underscoring that our comprehension of the precise mechanism that governs the triage of lipoproteins remains incomplete.

Excitingly, more unresolved questions regarding lipoprotein biogenesis have recently been raised. First, it was reported that a LolA-LolB-independent trafficking route to the outer membrane exists in *E. coli*[21], but the factors involved have remained unknown. Second, although lipoproteins have traditionally been considered to be exposed to the periplasm in *E. coli* and many other bacterial models[10], a series of investigations have started to challenge this view by identifying lipoproteins on the surface of *E. coli*, *Vibrio cholerae*, and *Salmonella* Typhimurium[22-24]. Overall, the field is beginning to explore a lipoprotein topological landscape that is more complex than previously assumed and raising intriguing questions about the signals that control surface targeting and exposure.

Here, stimulated by the hypothesis that crucial details of the mechanisms underlying lipoprotein maturation remained to be elucidated, we sought to identify novel molecular

determinants controlling lipoprotein biogenesis. First, we found that half of the outer membrane lipoproteins display a long and intrinsically disordered linker at their N-terminus. Intrigued by these unstructured segments, we probed their importance for the biogenesis of RcsF, NlpD, and Pal, three unrelated outer membrane lipoproteins. Unexpectedly, we found that deleting the linker altered the targeting of all three lipoproteins to the outer membrane. Focusing on RcsF, we determined that both the length and disordered character of the linker were important; we also found that the linker is required for optimal processing by Lol. Our observations reveal the unsuspected role played by protein intrinsic disorder in lipoprotein cellular localization. We also propose a model in which disordered linkers are important for targeting and/or displaying lipoproteins on the cell surface.

Results

Half of lipoproteins present N-terminal disordered segments

In an attempt to discover novel molecular determinants controlling the cellular localization of lipoproteins, we decided to systematically analyze the sequence of the lipoproteins encoded by the *E. coli* genome (strain MG1655) in search of unidentified structural features. *E. coli* encodes ~80 validated lipoproteins[25], of which 58 have been experimentally shown to localize in the outer membrane[26]. Comparative modeling of existing X-ray, cryogenic electron microscopy (cryo-EM), and nuclear magnetic resonance (NMR) structures revealed that approximately half of these outer membrane lipoproteins display a long segment (>22 residues) that is predicted to be disordered at the N-terminus (**Fig. 1, Extended Data Fig. 1, Supplementary Data Table 1**). In contrast, only one of the 8 lipoproteins that remain in the inner membrane (DcrB; **Extended Data Fig. 1., Supplementary Data Table 1**) had a long, disordered linker, suggesting that disordered peptides may be important for lipoprotein sorting.

Linker deletion perturbs outer membrane targeting

Intrigued by the presence of these N-terminal disordered segments in so many outer membrane lipoproteins, we decided to investigate their functional importance. We selected three structurally unrelated lipoproteins whose function could easily be assessed: the stress sensor RcsF (which triggers the Rcs signaling cascade when damage occurs in the envelope[27]), NlpD (which activates the periplasmic N-acetylmuramyl-L-alanine amidase AmiC, which is involved in peptidoglycan cleavage during cell division[28]), and the peptidoglycan-binding lipoprotein Pal (which is important for outer membrane constriction during cell division[29]).

We began by preparing truncated versions of RcsF, NlpD, and Pal devoid of their N-terminal unstructured linkers (**Supplementary Data Fig. 1b, Extended Data Fig. 1;** $RcsF_{\Delta 19-47}$, $Pal_{\Delta 26-56}$, and $NlpD_{\Delta 29-64}$). Note that the lipidated cysteine residue (+1) and the Lol sorting signal (the amino acids at positions +2 and +3) were not altered in $RcsF_{\Delta 19-47}$, $Pal_{\Delta 26-56}$, and $NlpD_{\Delta 29-64}$, nor in any of the constructs discussed below except in $RcsF_{CDD}$ (**Supplementary Data Table 2**). For Pal, although the unstructured linker spans residues 25-68 (**Fig. 1**), we used $Pal_{\Delta 26-56}$ because $Pal_{\Delta 25-68}$ was either degraded or not detected by the antibody. We first tested whether the truncated lipoproteins were still correctly extracted from the inner /and transported to the outer membrane. The membrane fraction was prepared from cells expressing the three variants independently, and the outer and inner membranes were separated using sucrose density gradients (Methods). Whereas wild-type RcsF, NlpD, and Pal were mostly detected (>90%) in the outer membrane fraction, ~50% of $RcsF_{\Delta 19-47}$ and ~60% of $NlpD_{\Delta 29-64}$ were retained in the inner membrane (**Fig. 2a, Extended Data Fig. 2a**). An RcsF variant in which the Lol sorting signal was replaced by two aspartates ($RcsF_{CDD}$) was used as a control for inner membrane retention; as expected, $RcsF_{CDD}$ was mostly detected in the inner membrane (**Extended Data Fig. 3**). The sorting of Pal was also affected, but to a lesser extent: 15% of $Pal_{\Delta 26-56}$ was retained in the inner membrane (**Extended Data Fig. 2b**). Notably, the expression levels of the three linker-less variants were similar ($NlpD_{\Delta 29-64}$) or lower ($RcsF_{\Delta 19-47}$; $Pal_{\Delta 26-56}$) than those of the wild-type proteins (**Extended Data Fig. 4**), indicating that accumulation in the inner membrane did not result from increased protein abundance.

We then tested the impact of linker deletion on the function of these three proteins. In cells expressing $RcsF_{\Delta 19-47}$, the Rcs system was constitutively turned on (**Fig. 2b**); when RcsF accumulates in the inner membrane, it becomes available for interaction with IgaA, its downstream Rcs partner in the inner membrane[27,30]. Likewise, expression of $NlpD_{\Delta 29-64}$ did not

rescue the chaining phenotype (**Fig. 2c**)[31] exhibited by cells lacking both *nlpD* and *envC*, an activator of the amidases AmiA and AmiB[28]. Finally, $Pal_{\Delta 26-56}$ partially rescued the sensitivity of the *pal* mutant to SDS-EDTA that results from increased membrane permeability[32] (**Fig. 2d**). However, this observation needs to be considered with caution given that $Pal_{\Delta 26-56}$ seemed to be expressed at lower levels than wild-type Pal (**Extended Data Fig. 4**). Thus, preventing normal targeting of RcsF, NlpD and Pal to the outer membrane had functional consequences.

Unstructured artificial linkers do the job

The results above were surprising because they revealed that the normal targeting of RcsF, NlpD, and Pal to the outer membrane does not only require an appropriate Lol sorting signal, as proposed by the current model for lipoprotein sorting[10], but also the presence of an N-terminal linker. We selected RcsF, whose accumulation in the inner membrane can be easily tracked by monitoring Rcs activity[27] , to investigate the structural features of the linker controlling lipoprotein maturation; keeping as little as 10% of the total pool of RcsF molecules in the inner membrane is sufficient to fully activate Rcs[27].

We first tested whether changing the sequence of the N-terminal segment while preserving its disordered character still yielded normal targeting of the protein to the outer membrane. To that end, we prepared an RcsF variant in which the N-terminal linker was replaced by an artificial, unstructured sequence (**Supplementary Data Table 2, Extended Data Fig. 1, Extended Data Fig. 5**) of similar length and consisting mostly of Glycine-Serine repeats ($RcsF_{GS}$). Substituting the wild-type linker with this artificial sequence was remarkably well tolerated by RcsF: $RcsF_{GS}$ was targeted normally to the outer membrane (**Fig. 3a, Extended Data Fig. 1, Supplementary Data Fig. 2a**) and did not constitutively activate the stress system

(**Fig. 3b**). Thus, although $RcsF_{GS}$ has an N-terminus with a completely different primary structure, it behaved like the wild-type protein.

We then investigated whether the N-terminal linker required a minimal length for proper targeting and function. We therefore constructed two RcsF variants with shorter, unstructured, artificial linkers ($RcsF_{GS2}$ and $RcsF_{GS3}$, with linkers of 18 and 10 residues, respectively; **Supplementary Data Table 2**, **Extended Data Fig. 1, Extended Data Fig. 5**). Importantly, $RcsF_{GS2}$ and, to a greater extent, $RcsF_{GS3}$ did not properly localize to the outer membrane: the shorter the linker, the more RcsF remained in the inner membrane (**Fig. 3a, Extended Data Fig. 1, Supplementary Data Fig. 2a**). Consistent with the amount of $RcsF_{GS2}$ and $RcsF_{GS3}$ retained in the inner membrane, Rcs activation levels were inversely related to linker length (**Fig. 3b**).

The disordered character of the linker is crucial

Taken together, the results above demonstrated that the RcsF linker can be replaced with an artificial sequence lacking secondary structure, provided that it is of appropriate length. Next, we sought to directly probe the importance of having a disordered linker by replacing the RcsF linker with an alpha-helical segment 35 amino acids long from the periplasmic chaperone FkpA ($RcsF_{FkpA}$; **Supplementary Data Table 2, Extended Data Fig**. **1, Extended Data Fig. 5**). Introducing order at the N-terminus of RcsF dramatically impacted the protein distribution between the two membranes: $RcsF_{FkpA}$ was substantially retained in the inner membrane (**Fig. 3c, Supplementary Data Fig. 2b**) and constitutively activated Rcs (**Fig. 3d**). As alpha-helical segments are considerably shorter than unstructured sequences containing a similar number of amino acids, we also prepared an RcsF variant ($RcsF_{col}$) with a longer alpha helix from the helical segment of colicin Ia, which is 73 amino acids in length and also predicted to remain

folded in the $RcsF_{col}$ construct (**Supplementary Data Table 2, Extended Data Fig. 1, Extended Data Fig. 5**). However, doubling the size of the helix had no impact, with $RcsF_{col}$ behaving similarly to $RcsF_{FkpA}$ (**Fig. 3c, 3d, Supplementary Data Fig. 2b**). Together, these data demonstrate that having an N-terminal disordered linker downstream of the Lol sorting signal is required to correctly target RcsF to the outer membrane. The length of the linker is important, but the sequence is not, on the condition that the linker does not fold into a defined secondary structure.

A disordered linker is needed for optimal processing by Lol

Our finding that N-terminal disordered linkers function as molecular determinants of the targeting of lipoproteins to the outer membrane raised the question of whether these linkers work in a Lol-dependent or Lol-independent manner. To address this mechanistic question, we tested the impact of deleting *lpp* on the targeting of $RcsF_{\Delta 19\text{-}47}$. The lipoprotein Lpp, also known as the Braun lipoprotein, covalently tethers the outer membrane to the peptidoglycan and controls the size of the periplasm[33,34]. Being expressed at ~1 million copies per cell[35], Lpp is numerically the most abundant protein in *E. coli*. Thus, by deleting *lpp*, we considerably decreased the load on the Lol system by removing its most abundant substrate. Remarkably, *lpp* deletion partly rescued the targeting of $RcsF_{\Delta 19\text{-}47}$ to the outer membrane (**Fig. 4a**), indicating that the linker functions in a Lol-dependent manner and suggesting that accumulation of $RcsF_{\Delta 19\text{-}47}$ in the inner membrane results from a decreased ability of the Lol system to process the linker-less RcsF variant. In agreement with this idea, normal targeting of $NlpD_{\Delta 29\text{-}64}$ to the outer membrane was restored in cells lacking Lpp (**Fig. 4a**). $Pal_{\Delta 26\text{-}56}$ could not be tested because membrane fractionation failed with *lpp pal* double mutant cells whether or not they expressed $Pal_{\Delta 26\text{-}56}$ (the *lpp pal* double mutant is viable but highly mucoid).

To obtain further insights into the mechanism at play here, we next monitored whether linker deletion impacted the transfer of RcsF from LolA to LolB *in vitro*. LolA with a C-terminal His-tag was expressed in the periplasm of cells expressing wild-type RcsF or $RcsF_{\Delta 19\text{-}47}$ and purified to near homogeneity via affinity chromatography (Methods; **Extended Data Fig. 6**). Both $RcsF_{WT}$ and $RcsF_{\Delta 19\text{-}47}$ were detected in immunoblots of the fractions containing purified LolA (**Extended Data Fig. 6**), indicating that both proteins form a soluble complex with LolA and confirming that they use this chaperone for transport across the periplasm. LolB was expressed as a soluble protein in the cytoplasm and purified by taking advantage of a C-terminal Strep-tag; LolB, which has more affinity for lipoproteins than LolA [36], was then incubated with LolA-$RcsF_{WT}$ or LolA-$RcsF_{\Delta 19\text{-}47}$ and pulled-down using Strep-Tactin beads (Methods). As both $RcsF_{WT}$ and $RcsF_{\Delta 19\text{-}47}$ were detected in the LolB-containing pulled-down fractions (**Fig. 4b**), we conclude that both proteins were transferred from LolA to LolB. Thus, the linker is not required for the transfer of RcsF from LolA to LolB.

We then focused on the LolCDE ABC transporter in charge of extracting outer membrane lipoproteins and transferring them to LolA. The structure of LolCDE in complex with a lipoprotein substrate was recently reported[37]. Although most of the lipoprotein polypeptide chain is non-visible in the structure, the triacylated N-terminal cysteine could be found inside a channel located between the plane of the membrane and the periplasmic domains of LolC and LolD. We thus hypothesized that N-terminal flexible linkers might be important to limit clashes between the lipoprotein substrate and the periplasmic domains of LolC and LolD. To test whether having a disordered linker increases the efficiency of LolCDE in lipoprotein extraction, we monitored the impact of over-expressing all LolCDE components (**Extended Data Fig. 7a**) on the targeting of $RcsF_{\Delta 19\text{-}47}$ to the outer membrane. However, we found that over-expression of LolCDE had no effect (**Extended Data Fig. 7b**).

Finally, we tested whether linker deletion impacted the processing of $RcsF_{\Delta 19\text{-}47}$ by the enzymes involved in lipoprotein maturation (Lgt, LspA, and Lnt; **Supplementary Data Fig. 1a**). We found that overexpressing Lgt, LspA and Lnt had no impact on membrane targeting (**Extended Data Fig. 8**). Further, the immature forms of $RcsF_{\Delta 19\text{-}47}$ that accumulate when these enzymes are depleted (**Extended Data Fig. 9**) were not detected when these enzymes are expressed, indicating that deletion of the linker does not block the processing of $RcsF_{\Delta 19\text{-}47}$ by the enzymes of the maturation pathway. Thus, taken together, our results suggest that retention of $RcsF_{\Delta 19\text{-}47}$ in the inner membrane does not result from the impairment of a specific step, but rather from less efficient processing of the truncated lipoprotein by the entire lipoprotein maturation pathway (see Discussion).

Are linkers important for surface exposure?

We noted that two of the lipoproteins under investigation here, Pal and RcsF, have been reported to be surface-exposed[27,38,39]. A topology model has been proposed to explain how RcsF reaches the surface: the lipid moiety of RcsF is anchored in the outer leaflet of the outer membrane while the N-terminal linker is exposed on the cell surface before being threaded through the lumen of β-barrel proteins[39]. Thus, in this topology, the linker allows RcsF to cross the outer membrane. It was therefore tempting to speculate that N-terminal disordered linkers may be used by lipoproteins as a structural device to cross the outer membrane and reach the cell surface. In addition, the accumulation of $RcsF_{\Delta 19\text{-}47}$ in the inner membrane **(Fig. 2a)** also suggests that Lol may be using N-terminal linkers to recognize lipoproteins destined to the cell surface before their extraction from the inner membrane in order to optimize their targeting to the machinery exporting them to their final destination (BAM in the case of RcsF[27,39,40]). To further investigate the link between disordered linkers and surface exposure, we tested whether

NlpD could be detected on the cell surface, which turned out to be the case (**Extended Data Fig. 10a**). In addition, we found that the N-terminal linker of BamC, a lipoprotein with access to the cell surface [41,42], is important for normal outer membrane targeting (**Extended Data Fig. 10b, 10c**).

Discussion

Lipoproteins are crucial for essential cellular processes such as envelope assembly and virulence. However, despite their functional importance and their potential as targets for new antibacterial therapies, we only have a vague understanding of the molecular factors that control their biogenesis. By discovering the role played by N-terminal disordered linkers in lipoprotein sorting, this study adds an important new layer to our comprehension of lipoprotein biogenesis in Gram-negative bacteria. Critically, it also indicates that the current model of lipoprotein sorting—that sorting between the two membranes is controlled by the 2 or 3 residues that are adjacent to the lipidated cysteine—needs to be revised. Lipoproteins with unstructured linkers at their N-terminus are commonly found in Gram-negative bacteria including many pathogens (see below); further work will be required to determine whether these linkers control lipoprotein targeting in organisms other than *E. coli*, laying the foundation for designing new antibiotics.

It was previously shown that both *lolA* and *lolB* (but not *lolCDE*) can be deleted under specific conditions[21], suggesting at least one alternate route for the transport of lipoproteins across the periplasm and their delivery to the outer membrane. During this investigation, we envisaged the possibility that the linker could be required to transport lipoproteins via a yet-to-be-identified pathway independent of LolA/LolB. However, our observations that both RcsF and $RcsF_{\Delta 19\text{-}47}$ were found in complex with LolA **(Extended Data Fig. 6)** and were transferred by LolA to LolB **(Fig. 4b)** does not support this hypothesis. Instead, our data clearly indicate that lipoproteins with N-terminal linkers still depend on the Lol system for extraction from the inner membrane and transport to the outer membrane **(Supplementary Data Fig. 1a)**; they also suggest that N-terminal linkers improve lipoprotein processing by Lol (see below).

The general view is that outer membrane lipoproteins remain oriented toward the periplasm. Excitingly, a series of reports have started to challenge this paradigm by identifying surface-exposed lipoproteins in *E. coli* and other bacteria [22,23]. By showing that four surface-exposed lipoproteins (RcsF, Pal, NlpD, BamC) have an N-terminal linker that is important for outer membrane targeting, our results also support a model in which N-terminal disordered linkers are important for displaying lipoproteins on the cell surface. Investigating whether a dedicated Lol-dependent route exists for surface-exposed lipoproteins will be the subject of future research. It is worth noting that N-terminal linkers are commonly found in lipoproteins expressed by the pathogens *Borrelia burgdorferi* and *Neisseria meningitidis*[23,43]; lipoprotein surface exposure is common in these pathogens.

Our work also delivers crucial insights into the functional importance of disordered segments in proteins in general. Most proteins are thought to present portions that are intrinsically disordered. For instance, it is estimated that 30-50% of eukaryotic proteins contain regions that do not adopt a defined secondary structure *in vitro*[44]. However, demonstrating that these unstructured regions are functionally important *in vivo* is challenging. By showing that an N-terminal disordered segment downstream of the Lol signal is required for the correct sorting of lipoproteins, our work provides direct evidence that evolution has selected intrinsic disorder by function.

In conclusion, the data reported here establish that the triage of lipoproteins between the inner and outer membranes is not solely controlled by the Lol sorting signal; additional molecular determinants, such as protein intrinsic disorder, are also involved. Our data further highlight

the previously unrecognized heterogeneity of the important lipoprotein family and call for a careful evaluation of the maturation pathways of these lipoproteins.

DATA AVAILABILITY

All data generated or analysed during this study are included in this published article and its supplementary information file.

REFERENCES

1. Silhavy, T.J., Kahne, D. & Walker, S. The bacterial cell envelope. *Cold Spring Harb Perspect Biol* **2**, a000414 (2010).
2. Weiner, J.H. & Li, L. Proteome of the Escherichia coli envelope and technological challenges in membrane proteome analysis. *Biochim Biophys Acta* **1778**, 1698-713 (2008).
3. Ricci, D.P. & Silhavy, T.J. Outer Membrane Protein Insertion by the β-barrel Assembly Machine. *EcoSal Plus* **8**, 0035-2018 (2019).
4. El Rayes, J., Rodríguez-Alonso, R. & Collet, J.F. Lipoproteins in Gram-negative bacteria: new insights into their biogenesis, subcellular targeting and functional roles. *Curr Opin Microbiol* **61**, 25-34 (2021).
5. Chimalakonda, G. et al. Lipoprotein LptE is required for the assembly of LptD by the beta-barrel assembly machine in the outer membrane of Escherichia coli. *Proc Natl Acad Sci U S A* **108**, 2492-7 (2011).
6. Sherman, D.J. et al. Lipopolysaccharide is transported to the cell surface by a membrane-to-membrane protein bridge. *Science* **359**, 798-801 (2018).
7. Malinverni, J.C. et al. YfiO stabilizes the YaeT complex and is essential for outer membrane protein assembly in Escherichia coli. *Mol Microbiol* **61**, 151-64 (2006).
8. Laloux, G. & Collet, J.F. "Major Tom to ground control: how lipoproteins communicate extra-cytoplasmic stress to the decision center of the cell". *J Bacteriol*, 00216-17 (2017).
9. Kovacs-Simon, A., Titball, R.W. & Michell, S.L. Lipoproteins of bacterial pathogens. *Infect Immun* **79**, 548-61 (2011).
10. Szewczyk, J. & Collet, J.F. The Journey of Lipoproteins Through the Cell: One Birthplace, Multiple Destinations. *Adv Microb Physiol* **69**, 1-50 (2016).
11. Babu, M.M. et al. A database of bacterial lipoproteins (DOLOP) with functional assignments to predicted lipoproteins. *J Bacteriol* **188**, 2761-73 (2006).
12. Narita, S.I. & Tokuda, H. Bacterial lipoproteins; biogenesis, sorting and quality control. *Biochim Biophys Acta Mol Cell Biol Lipids* **1862**, 1414-1423 (2017).
13. Horler, R.S., Butcher, A., Papangelopoulos, N., Ashton, P.D. & Thomas, G.H. EchoLOCATION: an in silico analysis of the subcellular locations of Escherichia coli proteins and comparison with experimentally derived locations. *Bioinformatics* **25**, 163-6 (2009).

14. Tokuda, H. & Matsuyama, S. Sorting of lipoproteins to the outer membrane in E. coli. *Biochim Biophys Acta* **1694**, IN1-9 (2004).
15. Gennity, J.M. & Inouye, M. The protein sequence responsible for lipoprotein membrane localization in Escherichia coli exhibits remarkable specificity. *J Biol Chem* **266**, 16458-64 (1991).
16. Terada, M., Kuroda, T., Matsuyama, S.I. & Tokuda, H. Lipoprotein sorting signals evaluated as the LolA-dependent release of lipoproteins from the cytoplasmic membrane of Escherichia coli. *J Biol Chem* **276**, 47690-4 (2001).
17. Hara, T., Matsuyama, S. & Tokuda, H. Mechanism underlying the inner membrane retention of Escherichia coli lipoproteins caused by Lol avoidance signals. *J Biol Chem* **278**, 40408-14 (2003).
18. Narita, S. & Tokuda, H. Amino acids at positions 3 and 4 determine the membrane specificity of Pseudomonas aeruginosa lipoproteins. *J Biol Chem* **282**, 13372-8 (2007).
19. Lewenza, S., Mhlanga, M.M. & Pugsley, A.P. Novel inner membrane retention signals in Pseudomonas aeruginosa lipoproteins. *J Bacteriol* **190**, 6119-25 (2008).
20. Lorenz, C., Dougherty, T.J. & Lory, S. Correct Sorting of Lipoproteins into the Inner and Outer Membranes of Pseudomonas aeruginosa by the Escherichia coli LolCDE Transport System. *mBio* **10**, 00194-19 (2019).
21. Grabowicz, M. & Silhavy, T.J. Redefining the essential trafficking pathway for outer membrane lipoproteins. *Proc Natl Acad Sci U S A* **114**, 4769-4774 (2017).
22. Wilson, M.M. & Bernstein, H.D. Surface-Exposed Lipoproteins: An Emerging Secretion Phenomenon in Gram-Negative Bacteria. *Trends Microbiol* **24**, 198-208 (2016).
23. Zuckert, W.R. Secretion of bacterial lipoproteins: through the cytoplasmic membrane, the periplasm and beyond. *Biochim Biophys Acta* **1843**, 1509-16 (2014).
24. Pride, A.C., Herrera, C.M., Guan, Z., Giles, D.K. & Trent, M.S. The outer surface lipoprotein VolA mediates utilization of exogenous lipids by Vibrio cholerae. *MBio* **4**, e00305-13 (2013).
25. Gonnet, P., Rudd, K.E. & Lisacek, F. Fine-tuning the prediction of sequences cleaved by signal peptidase II: a curated set of proven and predicted lipoproteins of Escherichia coli K-12. *Proteomics* **4**, 1597-613 (2004).
26. Sueki, A., Stein, F., Savitski, M.M., Selkrig, J. & Typas, A. Systematic Localization of Escherichia coli Membrane Proteins. *mSystems* **5**, 00808-19 (2020).
27. Cho, S.H. et al. Detecting Envelope Stress by Monitoring beta-Barrel Assembly. *Cell* **159**, 1652-64 (2014).
28. Uehara, T., Parzych, K.R., Dinh, T. & Bernhardt, T.G. Daughter cell separation is controlled by cytokinetic ring-activated cell wall hydrolysis. *EMBO J* **29**, 1412-22 (2010).
29. Gerding, M.A., Ogata, Y., Pecora, N.D., Niki, H. & de Boer, P.A. The trans-envelope Tol-Pal complex is part of the cell division machinery and required for proper outer-membrane invagination during cell constriction in E. coli. *Mol Microbiol* **63**, 1008-25 (2007).
30. Hussein, N.A., Cho, S.H., Laloux, G., Siam, R. & Collet, J.F. Distinct domains of Escherichia coli IgaA connect envelope stress sensing and down-regulation of the Rcs phosphorelay across subcellular compartments. *PLoS Genet* **14**, e1007398 (2018).

31. Tsang, M.J., Yakhnina, A.A. & Bernhardt, T.G. NlpD links cell wall remodeling and outer membrane invagination during cytokinesis in Escherichia coli. *PLoS Genet* **13**, e1006888 (2017).
32. Shrivastava, R., Jiang, X. & Chng, S.S. Outer membrane lipid homeostasis via retrograde phospholipid transport in Escherichia coli. *Mol Microbiol* **106**, 395-408 (2017).
33. Cohen, E.J., Ferreira, J.L., Ladinsky, M.S., Beeby, M. & Hughes, K.T. Nanoscale-length control of the flagellar driveshaft requires hitting the tethered outer membrane. *Science* **356**, 197-200 (2017).
34. Asmar, A.T. et al. Communication across the bacterial cell envelope depends on the size of the periplasm. *PLoS Biol* **15**, e2004303 (2017).
35. Li, G.W., Burkhardt, D., Gross, C. & Weissman, J.S. Quantifying absolute protein synthesis rates reveals principles underlying allocation of cellular resources. *Cell* **157**, 624-35 (2014).
36. Okuda, S. & Tokuda, H. Model of mouth-to-mouth transfer of bacterial lipoproteins through inner membrane LolC, periplasmic LolA, and outer membrane LolB. *Proc Natl Acad Sci U S A* **106**, 5877-82 (2009).
37. Tang, X. et al. Structural basis for bacterial lipoprotein relocation by the transporter LolCDE. *Nat Struct Mol Biol* **28**, 347-355 (2021).
38. Michel, L.V. et al. Dual orientation of the outer membrane lipoprotein Pal in Escherichia coli. *Microbiology* **161**, 1251-9 (2015).
39. Konovalova, A., Perlman, D.H., Cowles, C.E. & Silhavy, T.J. Transmembrane domain of surface-exposed outer membrane lipoprotein RcsF is threaded through the lumen of beta-barrel proteins. *Proc Natl Acad Sci U S A* **111**, E4350-8 (2014).
40. Rodriguez-Alonso, R. et al. Structural insight into the formation of lipoprotein-beta-barrel complexes. *Nat Chem Biol* **16**, 1019-1025 (2020).
41. Webb, C.T. & Lithgow, T. Identification of BamC on the Surface of E. coli. *Methods Mol Biol* **1329**, 215-25 (2015).
42. Webb, C.T. et al. Dynamic association of BAM complex modules includes surface exposure of the lipoprotein BamC. *J Mol Biol* **422**, 545-55 (2012).
43. Brooks, C.L., Arutyunova, E. & Lemieux, M.J. The structure of lactoferrin-binding protein B from Neisseria meningitidis suggests roles in iron acquisition and neutralization of host defences. *Acta Crystallogr F Struct Biol Commun* **70**, 1312-7 (2014).
44. Bardwell, J.C. & Jakob, U. Conditional disorder in chaperone action. *Trends Biochem Sci* **37**, 517-25 (2012).

ACKNOWLEDGMENTS

We thank Asma Boujtat for technical help. We are indebted to the members of the Collet laboratory and to Nassos Typas (EMBL, Heidelberg) for helpful suggestions and discussions and to Tom Silhavy (Princeton) and Nienke Buddelmeijer (Pasteur) for providing bacterial strains. J.S. was a research fellow of the FRIA and J.F.C. is an Investigator of the FRFS-WELBIO. This work was funded by the WELBIO (grant WELBIO-CR-20190-03), by grants from the F.R.S.-FNRS, from the Fédération Wallonie-Bruxelles (ARC 17/22-087), from the European Commission via the International Training Network Train2Target (721484), and from the EOS Excellence in Research Program of the FWO and FRS-FNRS (G0G0818N).

AUTHOR CONTRIBUTIONS

J.-F.C., J.E.R., J.S., and S.H.C. designed and performed the experiments. J.E.R., J.S., and S.H.C. constructed the strains and cloned the constructs. J.-F.C., J.E.R., J.S., S.H.C., and A.M. analyzed and interpreted the data. B.I.I. performed the structural analysis, M.D the microscopy analysis and N.C. the dot blot analysis. J.-F.C., J.E.R., and J.S. wrote the manuscript. All authors discussed the results and commented on the manuscript.

COMPETING INTERESTS

The authors declare no competing financial interests.

FIGURE LEGENDS

Figure 1. Structural analysis of lipoproteins reveals that half of outer membrane lipoproteins display an intrinsically disordered linker at the N-terminus.

The structures of the outer membrane lipoproteins RcsF, NlpD, Pal, and BamC were generated via comparative modeling (Methods). The 39 remaining lipoproteins are shown in **Extended Data Figure 1**. X-ray and cryo-EM structures are green, NMR structures are cyan, and structures built *via* comparative modeling from the closest analog in the same PFAM group are orange. In all cases, the N-terminal linker is magenta.

Figure 2. The N-terminal linker displayed by lipoproteins is important for outer membrane targeting.

a. The outer membrane (OM) and inner membrane (IM) were separated *via* centrifugation in a three-step sucrose density gradient (Methods). While $RcsF_{WT}$ was found predominantly in the OM, $RcsF_{\Delta 19\text{-}47}$ was substantially retained in the IM. Data are presented as the ratio of signal intensity in a single fraction to the total intensity in all fractions. All variants were expressed from plasmids (**Supplementary Data Table 4**). DsbD and Lpp were used as controls for the OM and IM, respectively. **b.** The Rcs system is constitutively active when the linker of RcsF is missing. Rcs activity was measured with a beta-galactosidase assay in a strain harboring a transcriptional *rprA::lacZ* fusion (Methods). All variants were expressed from a plasmid. Results were normalized to expression levels of the RcsF variants. Box-and-whiskers plots are shown from minimum to maximum with the central line that marks the median; first and third quartile with the whiskers are also shown; n = 6 biologically independent experiments. **c.** Phase-contrast images of the *envC::kan* Δ*nlpD* mutant complemented with $NlpD_{WT}$ or $NlpD_{\Delta 29\text{-}64}$. $NlpD_{\Delta 29\text{-}64}$ only partially rescues the chaining phenotype of the *envC::kan* Δ*nlpD*

double mutant. Scale bar, 5 µm. **d.** Expression of $Pal_{\Delta 26\text{-}56}$ does not rescue the sensitivity of the *pal::kan* mutant to SDS-EDTA. Cells were grown in LB medium at 37 °C until mid-log phase (OD_{600} = 0.5). Tenfold serial dilutions were made in LB, plated onto LB agar or LB agar supplemented with 0.01% SDS and 0.5 mM EDTA, and incubated at 37 °C. Images in **a**, **c**, and **d** are representative of biological triplicates. Graph in **a** was created by spline analysis of curves representing a mean of three independent experiments.

Figure 3. The length and the disordered character of the RcsF linker play key roles in RcsF targeting to the outer membrane.

a. The outer membrane (OM) and inner membrane (IM) were separated *via* centrifugation in a three-step sucrose density gradient (Methods). DsbD and Lpp were used as controls for the OM and IM, respectively. The longer the linker, the more protein was correctly translocated to the IM. All variants were expressed from plasmids (**Supplementary Data Table 4**). Aligned dot-plots are shown with a line at mean ± standard deviation of n = 3 biologically independent experiments. Images are representative of experiments and immunoblots performed in biological triplicate. **b.** Rcs activity was measured with a beta-galactosidase assay in a strain harboring a transcriptional *rprA::lacZ* fusion. All variants were expressed from a plasmid. Results were normalized to expression levels of RcsF variants. Box-and-whiskers plots are shown from minimum to maximum with the central line that marks the median; first and third quartile with the whiskers are also shown; n = 6 biologically independent experiments. Rcs activity relates to the quantity of RcsF retained in the inner membrane. **c.** RcsF mutants harboring alpha helical linkers ($RcsF_{FkpA}$ and $RcsF_{col}$) were subjected to two consecutive centrifugations in sucrose density gradients. Both mutants were inefficiently translocated from the IM to the OM. All variants are expressed from plasmids. Aligned dot-plots are shown with a line at mean ± standard deviation of n = 3 biologically independent experiments. Images are

representative of experiments and immunoblots performed in biological triplicate. **d.** The Rcs system was constitutively active in $RcsF_{FkpA}$ and $RcsF_{col}$ strains; activation levels were comparable to those of $RcsF_{\Delta 19\text{-}47}$. Rcs activity was measured as in **b**. Results were normalized as in **b**. Box-and-whiskers plots are shown from minimum to maximum with the central line that marks the median; first and third quartile with the whiskers are also shown; n = 6 biologically independent experiments.

Figure 4. N-terminal disordered linkers interact with the Lol system to target lipoproteins to the outer membrane.

a. Deleting Lpp rescues targeting of $RcsF_{\Delta 19\text{-}47}$ and $NlpD_{\Delta 29\text{-}64}$ to the outer membrane. The outer and inner membranes were separated *via* centrifugation in a sucrose density gradient (Methods). $RcsF_{\Delta 19\text{-}47}$ and $NlpD_{\Delta 29\text{-}64}$ accumulate in the inner membrane of cells expressing Lpp, the most abundant Lol substrate. Deletion of *lpp* improves their targeting to the outer membrane. Aligned dot-plots are shown with a line at mean ± standard deviation of n = 3 biologically independent experiments. The significance of differences among bacterial strains was assessed according to analysis of variance (ANOVA), followed by the application of Tukey's multiple comparison test. No adjustments were made for multiple comparison. RcsF variants were expressed from the chromosome and NlpD variants were expressed from a plasmid. **b.** *In vitro* pull-down experiments show that $RcsF_{WT}$ and $RcsF_{\Delta 19\text{-}47}$ are transferred from LolA to LolB. LolA-$RcsF_{WT}$ and LolA-$RcsF_{\Delta 19\text{-}47}$ complexes were obtained by LolA-His affinity chromatography followed by size exclusion chromatography (Methods). Each complex was incubated with LolB-Strep that was previously purified *via* Strep-Tactin affinity chromatography (Methods). Both RcsF variants were eluted in complex with LolB-strep, while LolA was only present in the flow through. I, input; FT, flow through; E, eluate. n = 3 biologically independent experiments.

METHODS

Bacterial growth conditions

Bacterial strains used in this study are listed in **Extended Data Table 3**. Bacterial cells were cultured in Luria broth (LB) at 37 °C unless stated otherwise. The following antibiotics were added when appropriate: spectinomycin (100 μg/mL), ampicillin (200 μg/mL), chloramphenicol (25 μg/mL), and kanamycin (50 μg/mL). L-arabinose (0.2%), isopropyl-β-D-thiogalactoside (IPTG; 20 μM to 1 mM) and L-fucose (0.2%) were used for induction or repression when appropriate.

Bacterial strains and plasmids

DH300 (a derivative of *Escherichia coli* MG1655 carrying a chromosomal *rprA*::*lacZ* fusion at the λ attachment site[45]) was used as wildtype throughout the study. All deletion mutants were obtained by transferring the corresponding alleles from the Keio collection[46] (kan^R) into DH300[45] via P1 phage transduction. Deletions were verified by PCR and the absence of the protein was verified *via* immunoblotting (when possible). If necessary, the kanamycin cassette was removed via site-specific recombination mediated by the yeast Flp recombinase with pCP20 vector[47]. All strains expressing the RcsF mutants used for subcellular fractionation lacked *rcsB* in order to prevent induction of Rcs.

The plasmids used in this study are listed in **Extended Data Table 4** and the primers appear in **Extended Data Table 5**. RcsF, Pal, and NlpD were expressed from the low-copy vector pAM238[48] containing the SC101 origin of replication and the *lac* promoter. To produce pSC202 for RcsF expression, *rcsF* (including approximately 30 base pairs upstream of the

599 coding sequence) was amplified by PCR from the chromosome of DH300 (primer pair
600 SH_RcsF(PstI)-R and SH_RcsFU-R (kpnI)-F). The amplification product was digested with
601 KpnI and PstI and inserted into pAM238, resulting in pSC202. *nlpD* was amplified using
602 primers JR1 and JR2 and *pal* was amplified with primers JS145 and JS146. Amplification
603 products were digested with PstI-XbaI and KpnI-XbaI, respectively, generating pJR8 (for
604 NlpD expression) and pJS20 (for Pal expression). To clone $rcsF_{\Delta 19\text{-}47}$, the nucleotides encoding
605 the RcsF signal sequence were amplified using primers SH_RcsFU-R(kpnI)_F and
606 SH_RcsFss-Fsg (NcoI)_R, and those encoding the RcsF signaling domain were amplified
607 using primers SH_RcsFss-Fsg (NcoI)_R and SH_RcsF(PstI)_R. In both cases, pSC202 was
608 used as template. Then, overlapping PCR was performed using SH_RcsFUR(kpnI)_F and
609 SH_RcsF(PstI)_R from the two PCR products previously obtained. The final product was
610 digested with KpnI and PstI, and ligated with pAM238 pre-digested with the same enzymes,
611 yielding pSC201. To add a GS linker (Ser-Gly-Ser-Gly-Ser-Gly-Ala-Met) into pSC201, the
612 primers SH_GS linker_F and SH_GS linker_R were mixed, boiled, annealed at room
613 temperature, and ligated with pSC201 pre-digested with NcoI, generating pSC198. pSC199
614 was generated similarly, but using primers SH_SG linker_F and SH_SG linker_R and plasmid
615 pSC198. pSC200 was generated using primers SH_Da linker_F and SH_SG linker_R and
616 plasmid pSC199.
617
618 $rcsF_{FkpA}$ and $rcsF_{col}$ were obtained by inserting DNA sequences corresponding to helical linker
619 fragments (FkpA Ser94-Glu125 and colicin IA Ile213-Lys282) into $rcsF_{\Delta 19\text{-}47}$ at NcoI and RsrII
620 restriction sites. The *fkpA* gene fragment was amplified from the *E. coli* MC4100 chromosome
621 (JS50/JS51 primers) and the *cia* gene fragment was chemically synthetized as a gene block by
622 Integrated DNA Technologies (IDT). The resulting plasmids were pJS18 and pJS27,
623 respectively. pAM238 does not contain the *lacIq* repressor. Therefore, to enable expression-

level regulation by IPTG, strains containing the pAM238 plasmids expressing RcsF variants were co-transformed with pET22b, a high-copy plasmid from a different incompatibility group (pBR223 origin of replication; Novagen) containing the *lacIq* repressor. Chromosomal insertion of $rcsF_{\Delta 19\text{-}47}$ or $rcsF_{CDD}$ at the *rcsF* locus was performed via λ-Red recombineering[49] with pSIM5-Tet plasmid (a gift of D. Hughes). In the first step, the *cat-sacB* cassette was introduced and later replaced by mutant *rcsF*. The same technique was used to add an HA tag to the chromosomal *fkpA* gene.

The *pal* allele lacking the linker region ($pal_{\Delta 26\text{-}56}$) was created *via* overlapping PCR. The pJS20 plasmid served as template for PCR with the M13R/M13F external primers and JS152/JS153 internal primers. The truncated allele was cloned into pAM238 at the same restriction sites as the full-length allele, producing pJS24. The *nlpD* allele lacking the linker regions ($nlpD_{\Delta 29\text{-}64}$) was created *via* overlapping PCR. *E. coli* chromosomal *nlpD* served as template for the PCR, with JR1/JR2 as external primers and JR7/JR8 as internal primers. The truncated allele was then cloned into pAM238 at the same restriction sites as the full-length allele, producing pJR10.

To clone $bamC_{WT}$ with a C-terminal Flag-tag, the chromosomal *bamC* gene was amplified by PCR using primers JR92 and JR93 and then inserted into pSC213, a modified IPTG-regulated pAM238 with a ribosome binding site and a C-terminal Flag-tag, previously digested with the restriction enzymes NcoI and XbaI, using the NEB Gibson master mix. To clone $bamC_{\Delta 28\text{-}98}$ with a C-terminal Flag-tag using pSC213, $bamC_{1\text{-}27}$ and $bamC_{99\text{-}344}$ were amplified by PCR using the chromosomal *bamC* gene and primers JR92/JR94 and JR95/JR96, respectively. pSC213 was digested using restriction enzymes NcoI and XbaI. $bamC_{\Delta 28\text{-}98}$ was then created by mixing PCR products ($bamC_{1\text{-}27}$ and $bamC_{99\text{-}344}$) with digested pSC213 and the NEB Gibson

master mix. $BamC_{WT}$ and $BamC_{\Delta 28\text{-}98}$ were induced using 20 µM and 40 µM of IPTG, respectively (**Extended Data Figure 10**).

The chromosomal *lolCDE* operon was amplified *via* PCR using primers JS277 and JS278 (adding a C-terminal His-tag to LolE) and then inserted into pBAD33 using the restriction sites PstI and XbaI, resulting in pJR203. The expression level of LolE-His was verified *via* immunoblotting.

The sequence encoding *lolB* without its N-terminal cysteine was first amplified from the chromosome *via* PCR using primers JR50/PL387 (adding a C-terminal Strep-tag). It was then cloned into pET28a using the restriction sites XbaI and PstI, generating plasmid pJR90. *lolA* was amplified using chromosomal *lolA* as PCR template for primers JR30/JR31 (JR31 contains the sequence of a His-tag) and then cloned into pBAD18 using KpnI and XbaI, resulting in pJR48.

The genes encoding Lgt and Lnt were amplified from the chromosome with PCR primers AG389/AG403 and AG393/JR74, respectively. AG403 and JR74 also encode a Myc-tag. PCR products were cloned into pAM238 using KpnI and PstI. Expression levels of the proteins constitutively expressed from the plasmid were verified *via* immunoblotting (**Extended Data Fig. 8**). *lspA* was amplified with PCR primers JR77/JR78. The PCR product was cloned into pSC213, a modified IPTG-regulated pAM238 with a ribosome binding site and a C-terminal Flag-tag, using NcoI and XbaI. Expression of LspA-Flag was induced by adding 25 µM IPTG.

Cell fractionation and sucrose density gradients

Cell fractionation was performed as described previously [50] with some modifications. Four hundred milliliters of cells were grown at 37°C in LB until the optical density at 600 nm (OD_{600}) of the culture reached 0.7. Cells were harvested *via* centrifugation at 6,000 x *g* at 4 °C for 15 min, washed with TE buffer (50 mM Tris-HCl pH 8, 1 mM EDTA), and resuspended in 20 mL of the same buffer. The washing step was skipped with the *Δlpp* strains to prevent the loss of outer membrane vesicles. DNase I (1 mg, Roche), RNase A (1 mg, Thermo Scientific), and a half tablet of a protease inhibitor cocktail (cOmplete EDTA-free Protease Inhibitor Cocktail tablets; Roche) were added to cell suspensions, and cells were passed through a French pressure cell at 1,500 psi. After adding $MgCl_2$ to a final concentration of 2 mM, the lysate was centrifuged at 5,000 x *g* at 4 °C for 15 min in order to remove cell debris. Then, 16 mL of supernatant were placed on top of a two-step sucrose gradient (2.3 mL of 2.02 M sucrose in 10 mM HEPES pH 7.5 and 6.6 mL of 0.77 M sucrose in 10 mM HEPES pH 7.5). The samples were centrifuged at 180,000 x *g* for 3 h at 4 °C in a 55.2 Ti Beckman rotor. After centrifugation, the soluble fraction and the membrane fraction were collected. The membrane fraction was diluted four times with 10 mM HEPES pH 7.5. To separate the inner and the outer membranes, 7 mL of the diluted membrane fraction were loaded on top of a second sucrose gradient (10.5 mL of 2.02 M sucrose, 12.5 mL of 1.44 M sucrose, 7 mL of 0.77 M sucrose, always in 10 mM HEPES pH 7.5). The samples were then centrifuged at 112,000 x *g* for 16 h at 10 °C in a SW 28 Beckman rotor. Approximately 30 fractions of 1.5 mL were collected and odd-numbered fractions were subjected to SDS-PAGE, transferred onto a nitrocellulose membrane, and probed with specific antibodies. Graphs were created in GraphPad Prism 9 *via* spline analysis of the curves representing a mean of three independent experiments. Aligned dot-plots representing the outer and inner membrane percentages were created in GraphPad Prism 9 by measuring the area under the curve for each experiment.

Immunoblotting

Protein samples were separated *via* 10% or 4-12% SDS-PAGE (Life Technologies) and transferred onto nitrocellulose membranes (GE Healthcare Life Sciences). The membranes were blocked with 5% skim milk in 50 mM Tris-HCl pH 7.6, 0.15 M NaCl, and 0.1% Tween 20 (TBS-T). TBS-T was used in all subsequent immunoblotting steps. The primary antibodies were diluted 5,000 to 20,000 times in 1% skim milk in TBS-T and incubated with the membrane for 1 h at room temperature. The anti-RcsF, anti-DsbD, anti-Lpp and anti-NlpD antisera were generated by our lab. These antibodies were used at 1/20,000, 1/9,000, 1/7,000 and 1/10,000, respectively. Anti-Pal, used at 1/20,000, was a gift from R. Lloubès and anti-His, used at 1/10,000, is a peroxidase-conjugated antibody (Qiagen). Anti-HA (Biolegend MMS-101R), used at 1/1,000, and anti-Flag (Sigma), used at 1/10,000, are mouse antisera while anti-Myc (Santa Cruz Biotechnology), used at 1/7,000, is a rabbit antiserum. The membranes were incubated for 1 h at room temperature with horseradish peroxidase-conjugated goat anti-rabbit IgG or anti-mouse (Sigma) at a 1:10,000 dilution. Labelled proteins were detected *via* enhanced chemiluminescence (Pierce ECL Western Blotting Substrate, Thermo Scientific) and visualized using X-ray film (Fuji) or a camera (Image Quant LAS 4000 and Vilber Fusion solo S). In order to quantify proteins levels, band intensities were measured using ImageJ version 1.46r (National Institutes of Health).

Testing the surface exposure of NlpD using dot-blots

The dot-blot method was adapted from [27]. Cells were grown in LB medium to an OD_{600} of 0.5. Cells were directly fixed for 15 min at room temperature with 0.04 % glutaraldehyde and 2 % formaldehyde. 2 x 1 mL of cells were centrifuged for 1 min at 16,000 x *g*. Fixed cells were resuspended in PBS. For permeabilization, cells were incubated for 30 min at 4°C in a buffer containing lysozyme (1 mg/mL) and EDTA (10 mM). After centrifugation, they were

resuspended in PBS. Cells (2 ml) were then spotted on nitrocellulose membranes and the spots were left to dry completely. The membranes were blocked for 30 min with 5 % (w/v) skim milk in TBS. Membranes were washed 5 min in TBS-Tween 20 0.05 % (TBS-T 0.05 %) and then incubated for 1 h at room temperature with primary antibody solutions. The anti-NlpD antibody was diluted 3,000 times with 1 % skim milk in TBS. Anti-HA mouse antibody (Biolegend MMS-101R) was diluted 1,000 times in BSA 2 % in TBS. Membranes were washed 3 times 5 min in TBS-T 0.05 % and incubated for 1 h at room temperature with secondary antibody solutions: anti-rabbit-HRP (Cytiva NA934) or anti-mouse-HRP (Sigma A4416) diluted 2,000 times with skim milk 5 % in TBS. Membranes were washed three times 5 min in TBS-T 0.05 %. Labeled proteins were detected with standard ECL or Substrate HRP Immobilon (Millipore) and visualized with a CCD camera.

β-galactosidase assay

β-galactosidase activity was measured as described previously[51]. Briefly, cells harboring P*rprA-lacZ* at the *att*B phage lambda site on the chromosome were diluted 1:100 from over-night cultures in LB, then incubated at 37°C and harvested at OD_{600} = 0.6. 20 µL of cells were harvested and incubated with 80 µL of permeabilization solution (60 mM $Na_2HPO_4 \cdot 2H_2O$, 40 mM $NaH_2PO_4 \cdot H_2O$, 10 mM KCl, 1 mM $MgSO_4 \cdot 7H_2O$, 50 mM β-mercaptoethanol) for 45 min at room temperature. Then, 600 µL of substrate (1 mg/mL O-nitrophenyl-β-d-galactoside, 50 mM β-mercaptoethanol) were added. The mixture was further incubated at 30°C for 20-90 min. The reaction was then stopped by adding 700 µL of 1 M Na_2CO_3 and absorbance was measured at 420 nm. The standardized amount of galactosidase activity was reported in Miller units. The ration of P*rprA-lacZ* induction was calculated relative to the basal level in a WT strain. Expression-level estimations were performed as follows. Cultures used for β-galactosidase activity (0.5 mL per culture) were precipitated with 10% trichloroacetic acid, washed with ice-

cold acetone, and resuspended in 0.2 mL Laemmli SDS sample buffer. Samples (5 µL) were subjected to SDS-PAGE and immunoblotted with anti-RcsF antibody. Box and whisker plots were prepared using GraphPad Prism 9.

SDS-EDTA sensitivity assay

Cells were grown in LB at 37 °C until they reached an OD_{600} of 0.7. Tenfold serial dilutions were made in LB and plated on LB agar supplemented with spectinomycin (100 µg/mL) when necessary. Plates were incubated at 37 °C. To evaluate the sensitivity of the *pal* mutant, plates were supplemented with 0.01% SDS and 0.5 mM EDTA.

Microscopy image acquisition

Cells were grown in LB at 37 °C until OD_{600} = 0.5. Cells growing in exponential phase were spotted onto a 1% agarose phosphate-buffered saline pad for imaging. Images were taken at 21°C. Cells were imaged on a Nikon Eclipse Ti2-E inverted fluorescence microscope with a CFI Plan Apochromat DM Lambda 100X Oil, N.A. 1.45, W.D. 0.13 mm objective. Images were collected on a Prime 95B 25 mm camera (Photometrics). We used a Cy5-4050C (32 mm) filter cube (Nikon). Image acquisition was performed with NIS-Element Advance Research version 4.5. Whole field pictures are 2048 x 2048 pixels, 1 pixel accounts for 0.11 x 0.11 µm. Exposure time for phase contrast images were taken for 70 ms with a 75 % light intensity with SOLA II shutter. Display range: 5402 – 11791.

Protein purification

JR90 cells were grown in LB supplemented with kanamycin (50 µg/mL) at 37 °C. When the culture OD_{600} reached 0.5, the expression of cytoplasmic LolB-Strep was induced with 1 mM IPTG. Cells (1 L) were pelleted when they reached OD_{600} = 3 and resuspended in 25 mL of

buffer A (200 mM NaCl and 50 mM NaPi, pH 8) containing one tablet of cOmplete EDTA-free Protease Inhibitor Cocktail (Roche). Cells were lysed *via* two passages through a French pressure cell at 1,500 psi. The lysate was centrifuged at 30,000 x *g* for 40 min at 4 °C in a JA 20 rotor and the supernatant was mixed with Strep-Tactin resin (IBA Lifesciences) previously equilibrated with buffer A. After washing the resin with 10 column volumes of buffer A, LolB-Strep was eluted with 5 column volumes of buffer A supplemented with 5 mM desthiobiotin. LolB-Strep was finally desalted using a PD10 column (GE Healthcare).

Soluble LolA-RcsF$_{WT}$ and LolA-RcsF$_{\Delta 19\text{-}47}$ complexes were purified *via* affinity chromatography as follows. Cells co-expressing LolA either with wild-type RcsF (JR47) or RcsF$_{\Delta 19\text{-}47}$ (JR44) were grown in LB at 37 °C supplemented with 200 µg/mL ampicillin until an OD$_{600}$ of 0.5. Protein expression was then induced with 0.2% arabinose. Cells (1 L) were pelleted at an OD$_{600}$ of 3 and resuspended in 25 mL of buffer A containing one tablet of protease inhibitor cocktail. Cells were lysed *via* two passages through a French pressure cell at 1,500 psi. The lysate was centrifuged at 45,000 x *g* for 30 min at 4 °C using a 55.2 Ti Beckman rotor. To obtain the soluble fraction, the supernatant was centrifuged at 180,000 x *g* for 1 h at 4 °C using the same rotor. The supernatant was added to a His Trap HP column (Merck) previously equilibrated with buffer A. The column was washed with 10 column volumes of buffer A supplemented with 20 mM imidazole and LolA-His was eluted using a gradient of imidazole (from 20 mM to 300 mM). The fractions obtained were analyzed *via* SDS-PAGE; LolA was detected around 25 kDa. RcsF variants and LolA-His were detected *via* immunoblotting with an anti-RcsF and anti-His antibodies, respectively. Fractions containing LolA-RcsF variants were pooled, concentrated to 1 mL using a Vivaspin 4 Turbo concentrator (Cut-off 5 kDa; Sartorius), and purified *via* size-exclusion chromatography with a Superdex S75-10/300 column (GE Healthcare).

Pull down and transfer of RcsF variants from LolA to LolB

LolB-Strep was incubated at 30 °C for 20 min under agitation with LolA-$RcsF_{WT}$ or with LolA-$RcsF_{\Delta 19\text{-}47}$ (LolA-$RcsF_{WT}$ and LolA-$RcsF_{\Delta 19\text{-}47}$ complexes were purified as described above). The mixture was added to magnetic Strep beads (MagStrep type 3 beads, IBA Life science) previously equilibrated with buffer A and incubated for 30 min at 4 °C on a roller. After washing the beads with the same buffer, LolB-Strep was eluted with buffer A supplemented with 50 mM biotin. Samples were analyzed *via* SDS-PAGE and LolA and LolB were detected with Coomassie Brilliant Blue (Bio-Rad). RcsF was detected *via* immunoblotting with an anti-RcsF antibody.

Depletion of the maturation enzymes Lgt and Lnt

Lgt null strains (JR301 and JR302) expressing Lgt from an arabinose-inducible promoter on the pCHAP9231 plasmid[52] were prepared using P1 phage transduction from the Lgt null strain PAP9403 [52] (gift from N. Buddelmeijer, Pasteur, France). Overnight cultures were grown at 37°C in LB medium in the presence of 0.2 % arabinose (to allow expression of Lgt) and chloramphenicol (pCHAP9231 has chloramphenicol resistance). Cells were then diluted in fresh LB medium and grown at 37°C until growth arrest was observed and OD_{600} remained constant. Cells were then precipitated with 10 % trichloroacetic acid, washed with ice-cold acetone and resuspended in tricine SDS sample buffer. Samples were subjected to SDS-PAGE using tricine 16 % gel at 125 V, and immunoblotted with anti-Lpp and anti-RcsF antibodies.

The Lnt null strain PAP8504 [53] is a kind gift from N. Buddelmeijer. In PAP8504 strain, an arabinose inducible promoter controls the expression of the chromosomal *lnt* gene. Overnight precultures were grown at 37°C in LB medium in the presence of 0.2 % arabinose to allow the

822 expression of Lnt. Precultures were then washed three times with fresh LB medium and diluted
823 1:100 in LB supplemented with 0.2 % fucose. When growth arrest was observed and OD_{600}
824 remained constant, cells were precipitated as described previously. Samples were resuspended
825 in Tris-glycine SDS sample buffer and subjected to SDS-PAGE using Tris-glycine 16 % gel at
826 125 V, and immunoblotted with anti-Lpp and anti-RcsF antibodies. To monitor the impact of
827 Lnt depletion on $RcsF_{\Delta 19\text{-}47}$, plasmid pSC201 was introduced in PAP8504, yielding strain
828 JR320.
829
830 **Structural analysis of lipoproteins**
831 When X-ray, cryo-EM, or NMR structures were available, the missing residues were
832 completed through comparative modeling using MODELLER version 9.22[54]. If no structure of
833 the lipoprotein was available, then the most pertinent analogous structure from proteins
834 belonging to the same PFAM group was used as template for comparative modeling. The linker
835 was defined as the unstructured fragment from the N-terminal Cys of the mature form until the
836 first residue with well-defined secondary structure (α-helix or β-strand) belonging to a globular
837 domain. Short, intermediate, and long linkers had lengths of <12, 12-22, and >22 residues,
838 respectively. Images were generated using UCSF Chimera version 1.13.1[55].
839
840 **Statistical methods**
841 The significance of differences among bacterial strains was assessed using GraphPad Prism 9
842 according to analysis of variance (ANOVA), followed by the application of Tukey's multiple
843 comparison test.
844
845 45. Majdalani, N., Hernandez, D. & Gottesman, S. Regulation and mode of action of the
846 second small RNA activator of RpoS translation, RprA. *Mol Microbiol* **46**, 813-26
847 (2002).

46. Baba, T. et al. Construction of Escherichia coli K-12 in-frame, single-gene knockout mutants: the Keio collection. *Mol Syst Biol* **2**, 2006 0008 (2006).
47. Cherepanov, P.P. & Wackernagel, W. Gene disruption in Escherichia coli: TcR and KmR cassettes with the option of Flp-catalyzed excision of the antibiotic-resistance determinant. *Gene* **158**, 9-14 (1995).
48. Gil, D. & Bouche, J.P. ColE1-type vectors with fully repressible replication. *Gene* **105**, 17-22 (1991).
49. Yu, D. et al. An efficient recombination system for chromosome engineering in Escherichia coli. *Proc Natl Acad Sci U S A* **97**, 5978-83 (2000).
50. Sklar, J.G. et al. Lipoprotein SmpA is a component of the YaeT complex that assembles outer membrane proteins in Escherichia coli. *Proc Natl Acad Sci U S A* **104**, 6400-5 (2007).
51. Miller, J.C. *Experiments in Molecular Genetics*, (Cold Spring Harbor Laboratory Press, New York, 1972).
52. Pailler, J., Aucher, W., Pires, M. & Buddelmeijer, N. Phosphatidylglycerol::prolipoprotein diacylglyceryl transferase (Lgt) of Escherichia coli has seven transmembrane segments, and its essential residues are embedded in the membrane. *J Bacteriol* **194**, 2142-51 (2012).
53. Robichon, C., Vidal-Ingigliardi, D. & Pugsley, A.P. Depletion of apolipoprotein N-acyltransferase causes mislocalization of outer membrane lipoproteins in Escherichia coli. *J Biol Chem* **280**, 974-83 (2005).
54. Šali, A. & Blundell, T.L. Comparative Protein Modelling by Satisfaction of Spatial Restraints. *Journal of Molecular Biology* **234**, 779-815 (1993).
55. Pettersen, E.F. et al. UCSF Chimera - A visualization system for exploratory research and analysis. *Journal of Computational Chemistry* **25**, 1605-1612 (2004).

RcsF

NlpD

Pal

BamC

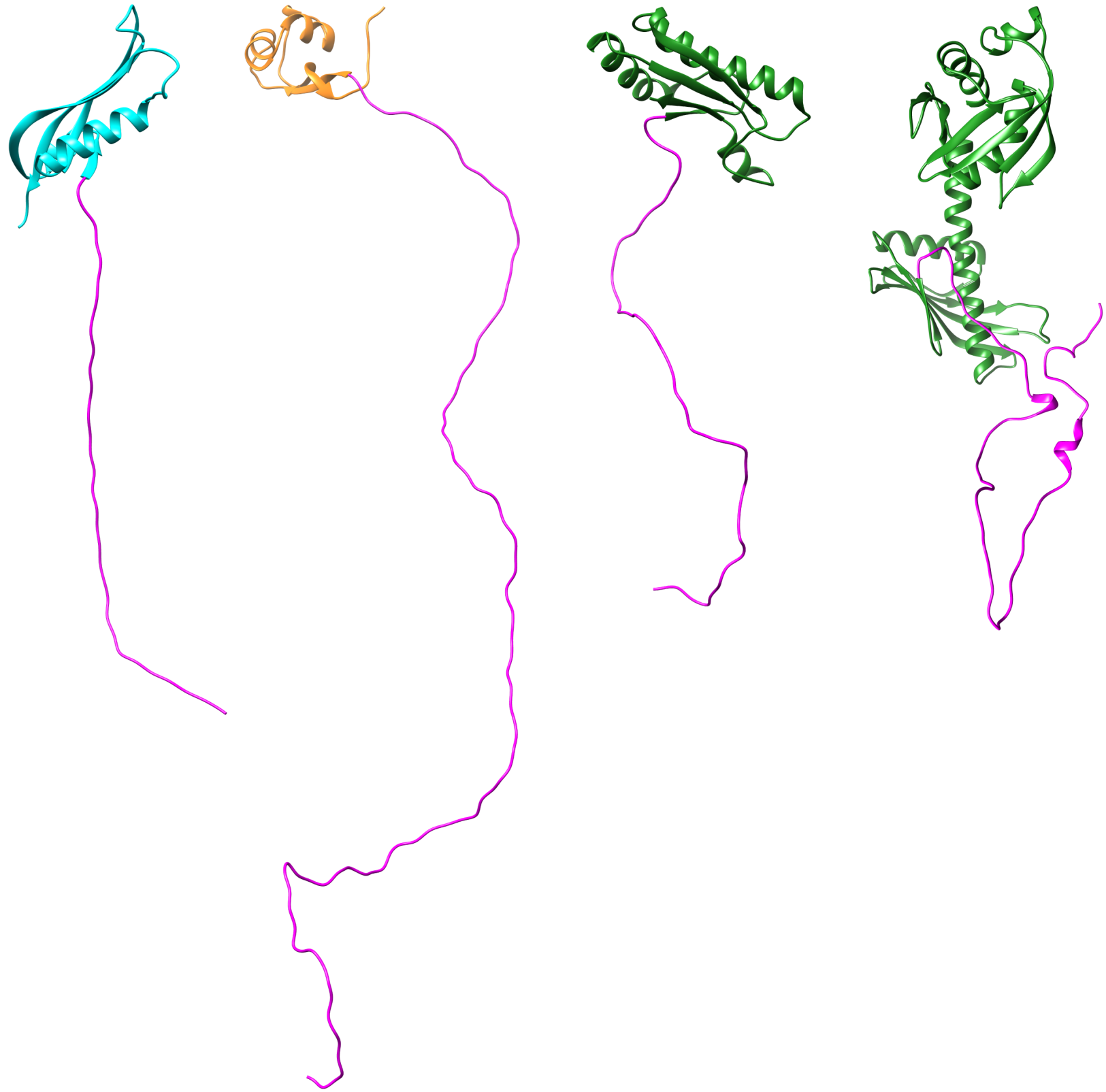

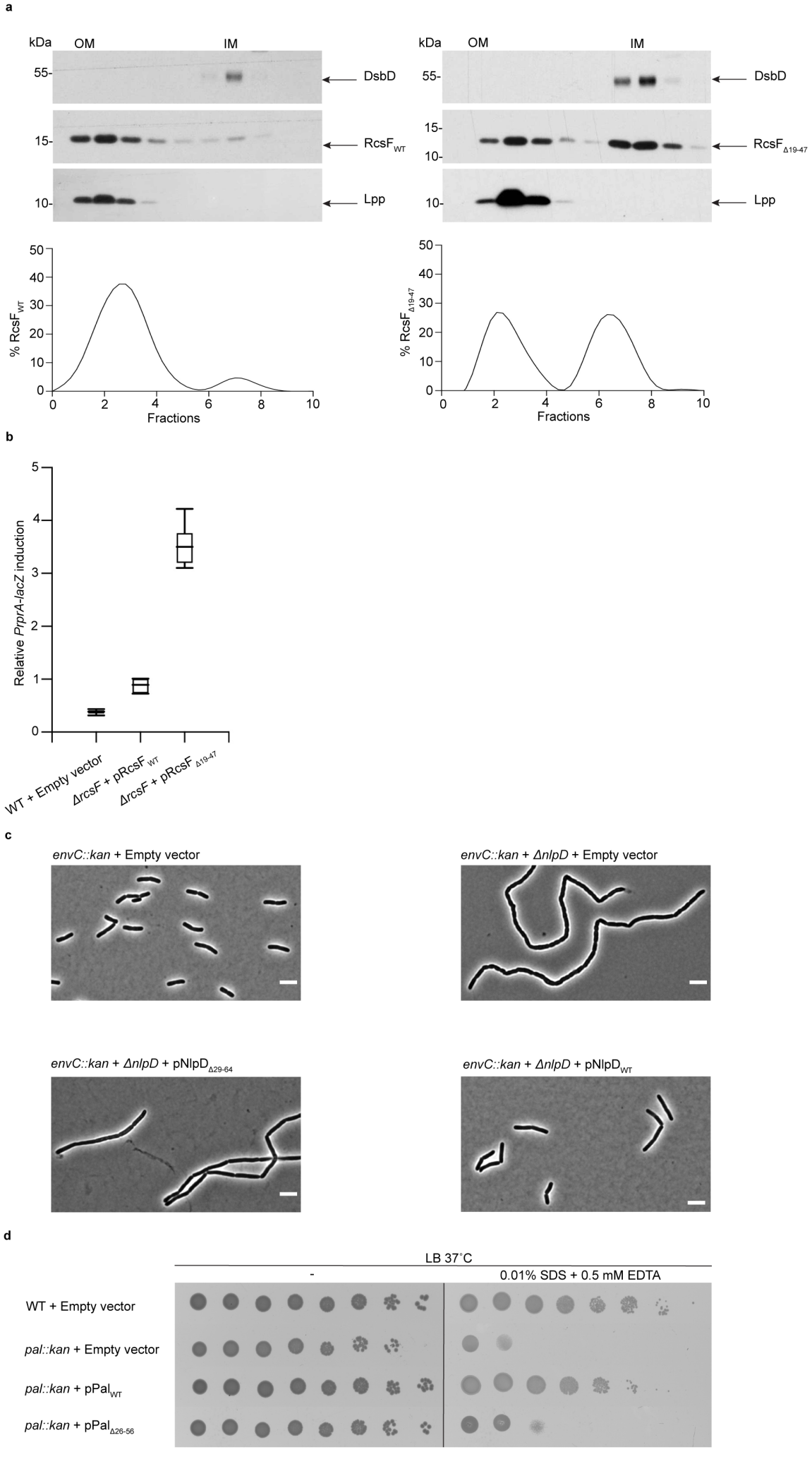
a
kDa
OM
IM
55-
DsbD
15-
RcsF$_{WT}$
10-
Lpp
% RcsF$_{WT}$
Fractions
RcsF$_{\Delta 19-47}$
% RcsF$_{\Delta 19-47}$
b
Relative *PprpA-lacZ* induction
WT + Empty vector
Δ*rcsF* + pRcsF $_{WT}$
Δ*rcsF* + pRcsF $_{\Delta 19-47}$
c
envC::kan + Empty vector
envC::kan + Δ*nlpD* + Empty vector
envC::kan + Δ*nlpD* + pNlpD$_{\Delta 29-64}$
envC::kan + Δ*nlpD* + pNlpD$_{WT}$
d
LB 37˚C
-
0.01% SDS + 0.5 mM EDTA
WT + Empty vector
pal::kan + Empty vector
pal::kan + pPal$_{WT}$
pal::kan + pPal$_{\Delta 26-56}$

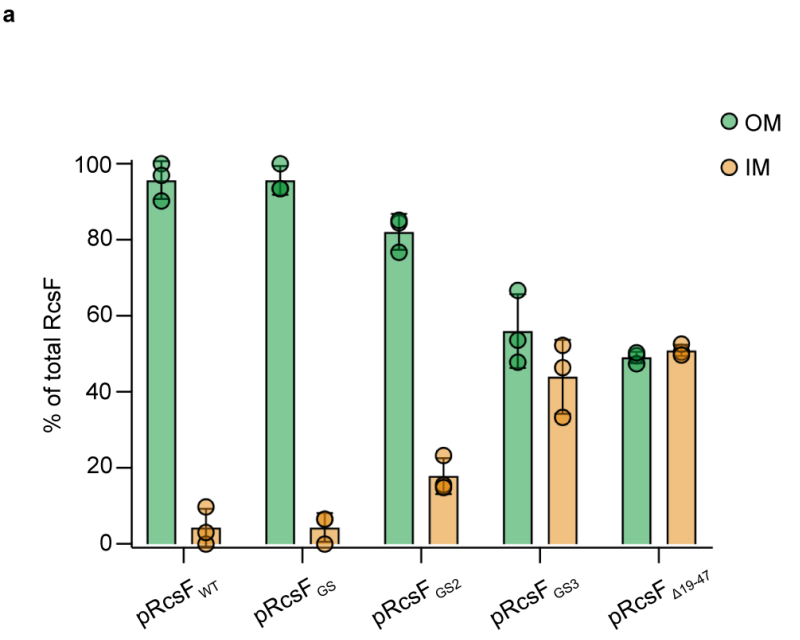
a
OM
IM
% of total RcsF
100
80
60
40
20
0
pRcsF WT
pRcsF GS
pRcsF GS2
pRcsF GS3
pRcsF Δ19-47

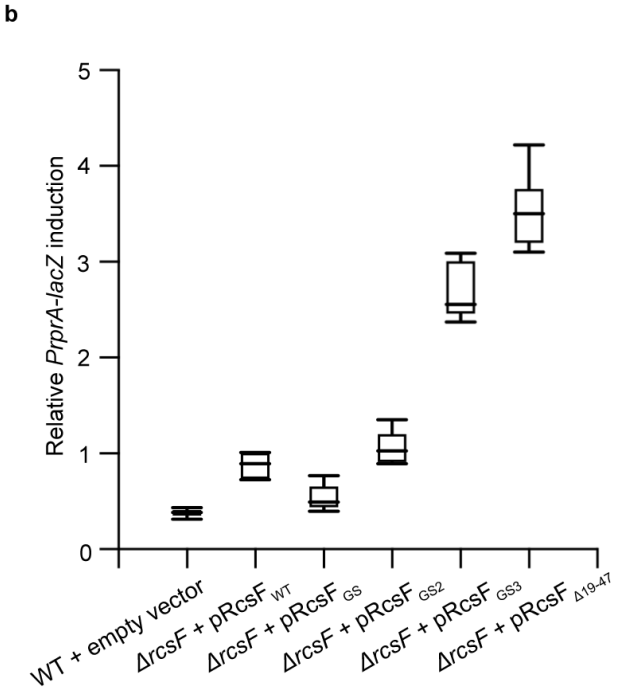
b
Relative PprrA-lacZ induction
5
4
3
2
1
0
WT + empty vector
ΔrcsF + pRcsF WT
ΔrcsF + pRcsF GS
ΔrcsF + pRcsF GS2
ΔrcsF + pRcsF GS3
ΔrcsF + pRcsF Δ19-47

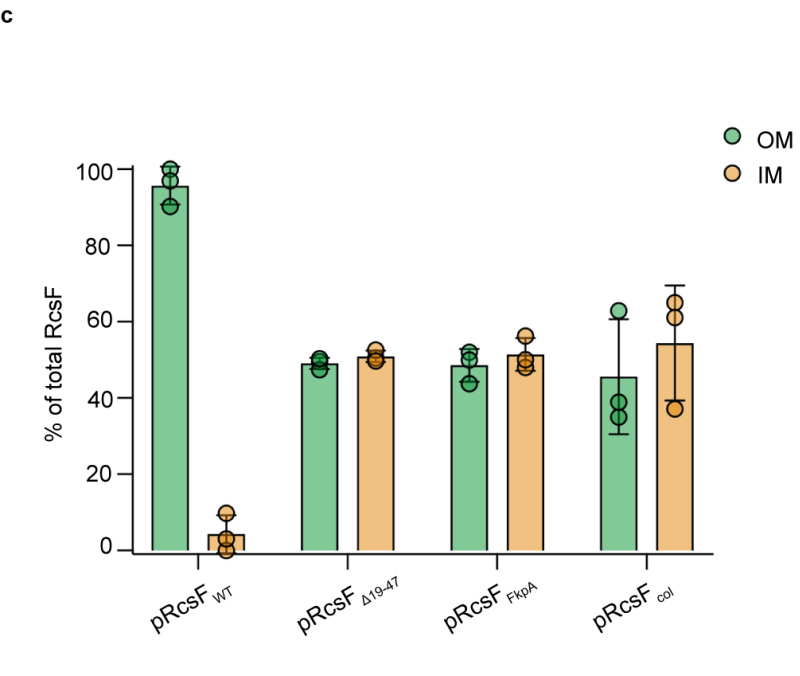
c
OM
IM
% of total RcsF
100
80
60
40
20
0
pRcsF WT
pRcsF Δ19-47
pRcsF FkpA
pRcsF col

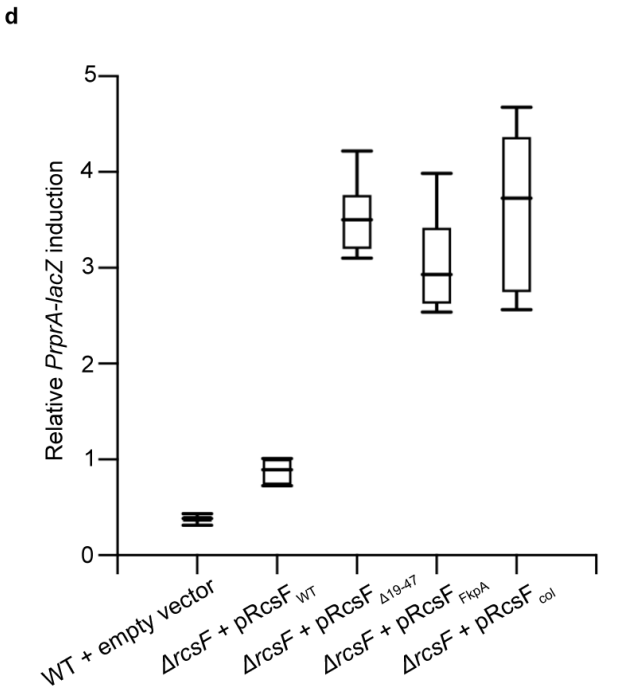
d
Relative PprrA-lacZ induction
5
4
3
2
1
0
WT + empty vector
ΔrcsF + pRcsF WT
ΔrcsF + pRcsF Δ19-47
ΔrcsF + pRcsF FkpA
ΔrcsF + pRcsF col

a

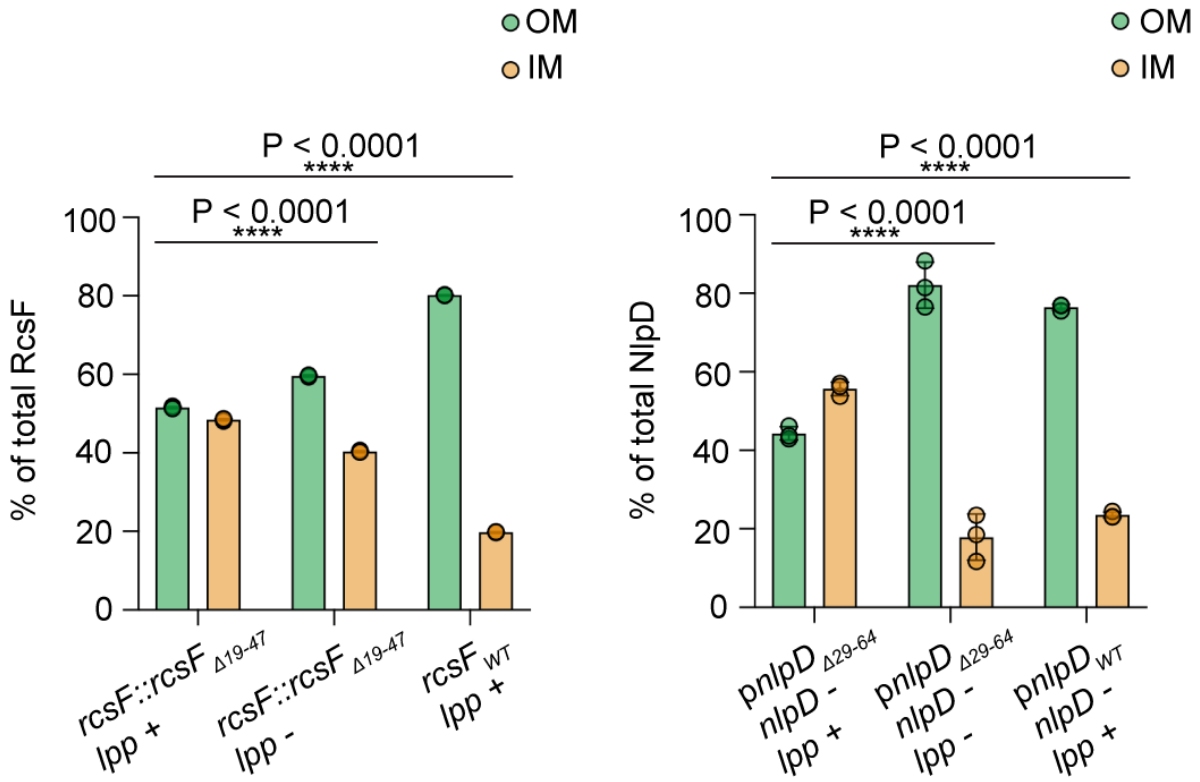
OM
IM
P < 0.0001
****
P < 0.0001
****
100
80
60
40
20
0
% of total RcsF
rcsF::rcsF Δ19-47 lpp +
rcsF::rcsF Δ19-47 lpp -
rcsF WT lpp +
OM
IM
P < 0.0001
****
P < 0.0001
****
100
80
60
40
20
0
% of total NlpD
pnlpD Δ29-64 nlpD - lpp +
pnlpD Δ29-64 nlpD - lpp -
pnlpD WT nlpD - lpp +

b

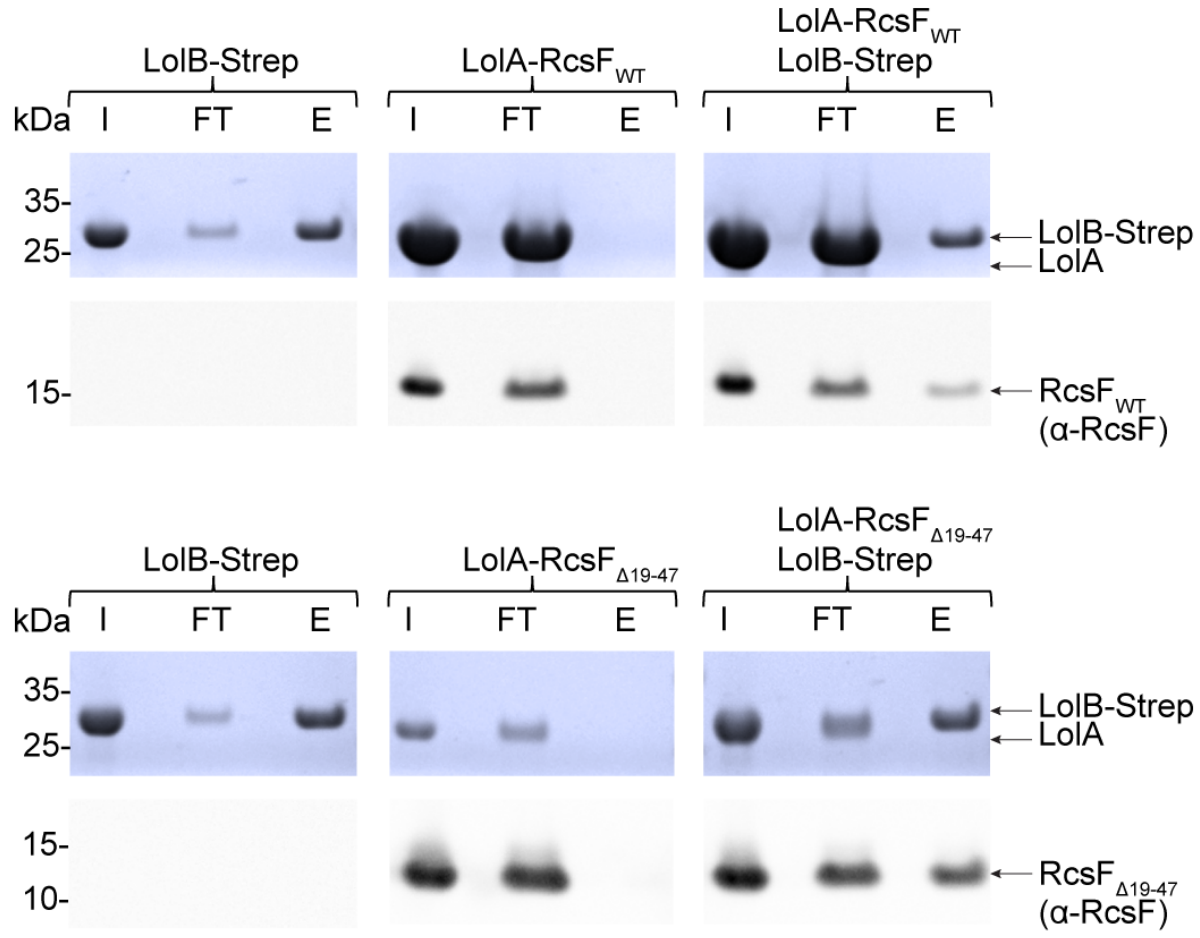
LolB-Strep
LolA-RcsF WT
LolA-RcsF WT LolB-Strep
kDa
I
FT
E
35-
25-
15-
LolB-Strep
LolA
RcsF WT (α-RcsF)
LolB-Strep
LolA-RcsF Δ19-47
LolA-RcsF Δ19-47 LolB-Strep
kDa
I
FT
E
35-
25-
15-
10-
LolB-Strep
LolA
RcsF Δ19-47 (α-RcsF)

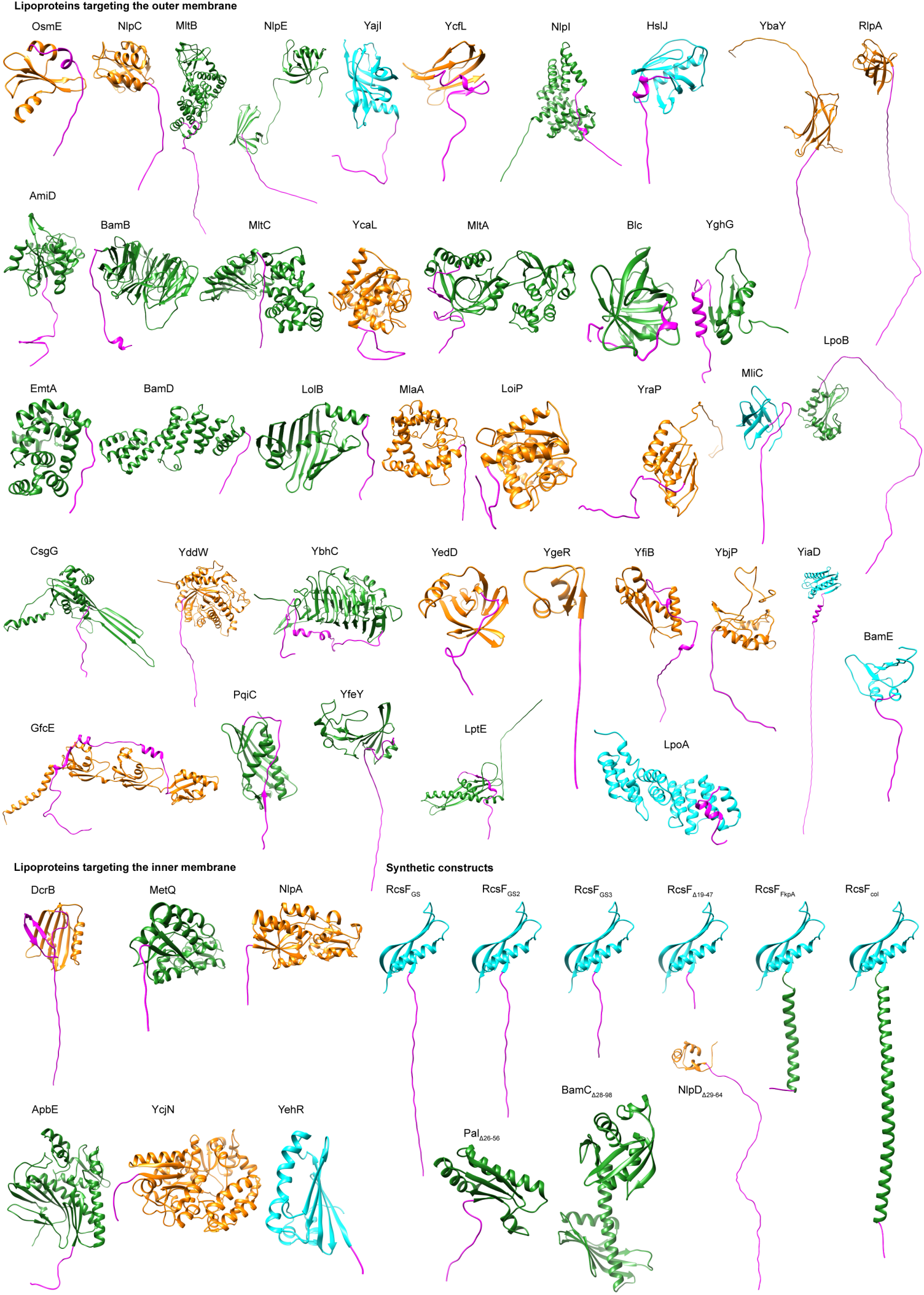
Lipoproteins targeting the outer membrane
OsmE
NlpC
MltB
NlpE
YajI
YcfL
NlpI
HslJ
YbaY
RlpA
AmiD
BamB
MltC
YcaL
MltA
Blc
YghG
LpoB
EmtA
BamD
LolB
MlaA
LoiP
YraP
MliC
CsgG
YddW
YbhC
YedD
YgeR
YfiB
YbjP
YiaD
BamE
PqiC
YfeY
GfcE
LptE
LpoA
Lipoproteins targeting the inner membrane
DcrB
MetQ
NlpA
ApbE
YcjN
YehR
Synthetic constructs
RcsF$_{GS}$
RcsF$_{GS2}$
RcsF$_{GS3}$
RcsF$_{\Delta 19-47}$
RcsF$_{FkpA}$
RcsF$_{col}$
BamC$_{\Delta 28-98}$
NlpD$_{\Delta 29-64}$
Pal$_{\Delta 26-56}$

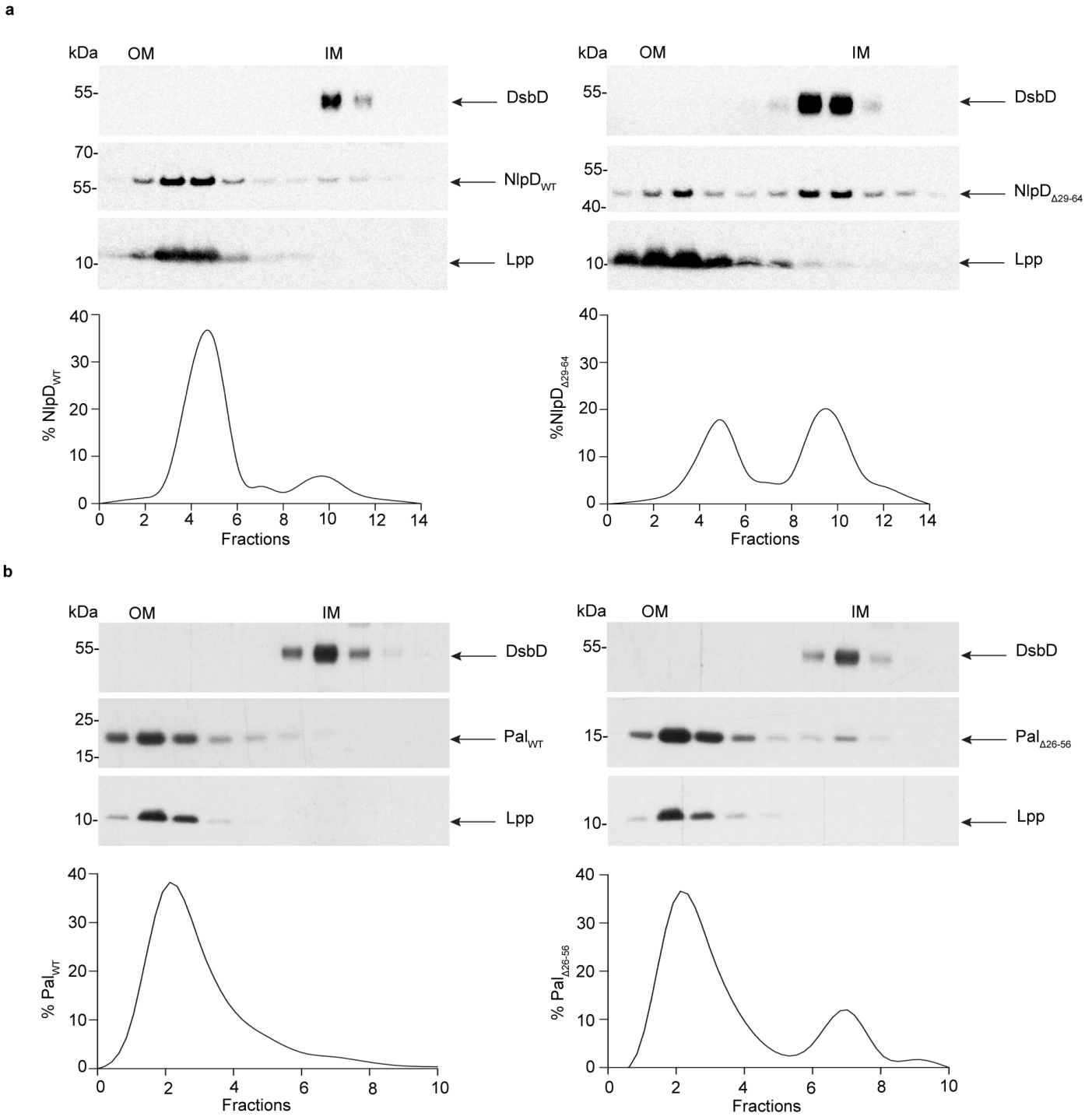
a
kDa
OM
IM
55-
DsbD
70-
55-
NlpD$_{WT}$
10-
Lpp
% NlpD$_{WT}$
Fractions
kDa
OM
IM
55-
DsbD
55-
40-
NlpD$_{\Delta 29-64}$
10-
Lpp
%NlpD$_{\Delta 29-64}$
Fractions
b
kDa
OM
IM
55-
DsbD
25-
15-
Pal$_{WT}$
10-
Lpp
% Pal$_{WT}$
Fractions
kDa
OM
IM
55-
DsbD
15-
Pal$_{\Delta 26-56}$
10-
Lpp
% Pal$_{\Delta 26-56}$
Fractions

a

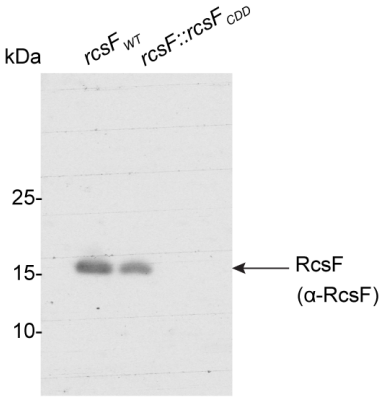
kDa
rcsF WT
rcsF::rcsF CDD
25-
15-
10-
RcsF
(α-RcsF)

b

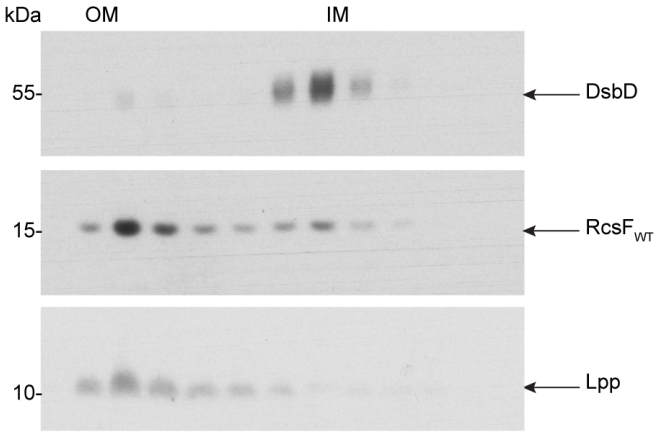
kDa
OM
IM
55-
15-
10-
DsbD
RcsF WT
Lpp

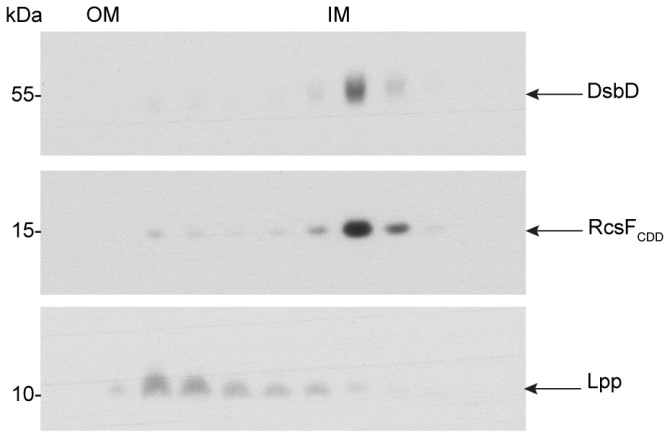
kDa
OM
IM
55-
15-
10-
DsbD
RcsF CDD
Lpp

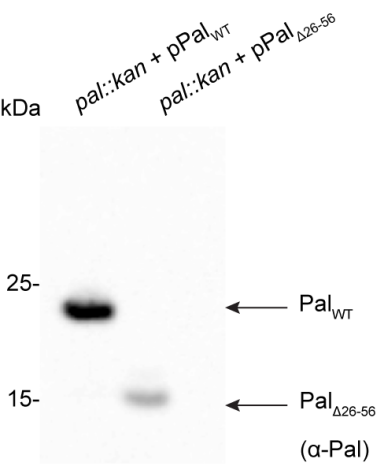
kDa
pal::kan + pPal WT
pal::kan + pPal Δ26-56
25-
15-
Pal WT
Pal Δ26-56
(α-Pal)

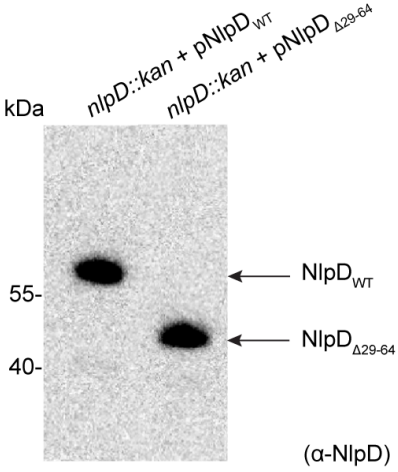
kDa
nlpD::kan + pNlpD WT
nlpD::kan + pNlpD Δ29-64
55-
40-
NlpD WT
NlpD Δ29-64
(α-NlpD)

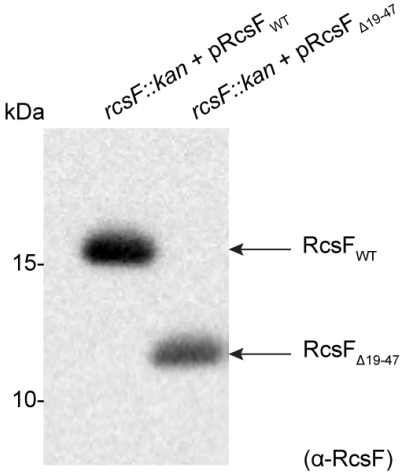
kDa
rcsF::kan + pRcsF WT
rcsF::kan + pRcsF Δ19-47
15-
10-
RcsF WT
RcsF Δ19-47
(α-RcsF)

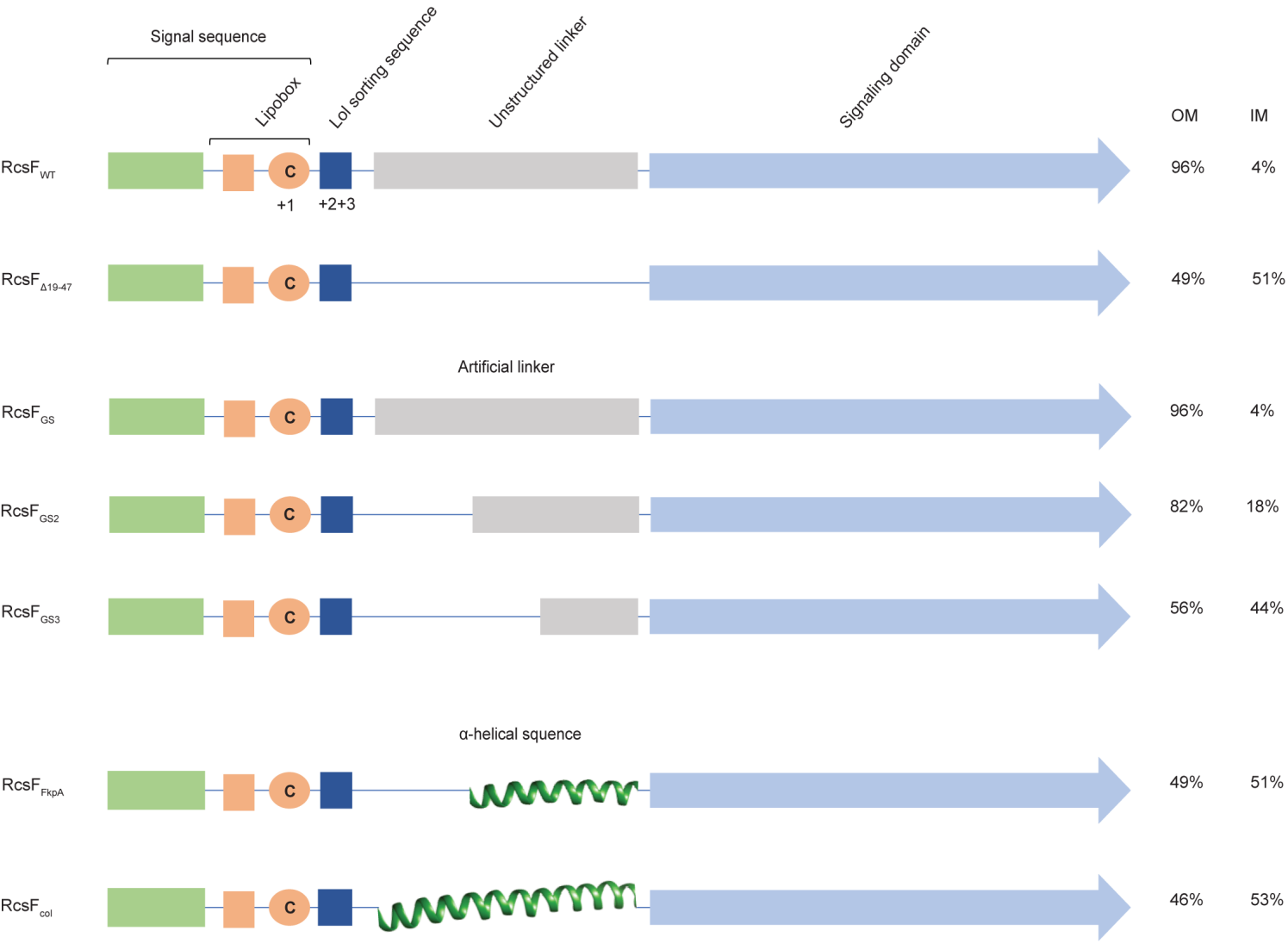
Signal sequence
Lipobox
Lol sorting sequence
Unstructured linker
Signaling domain
OM
IM
RcsF WT
C
+1
+2+3
96%
4%
RcsF Δ19-47
49%
51%
Artificial linker
RcsF GS
96%
4%
RcsF GS2
82%
18%
RcsF GS3
56%
44%
α-helical squence
RcsF FkpA
49%
51%
RcsF col
46%
53%

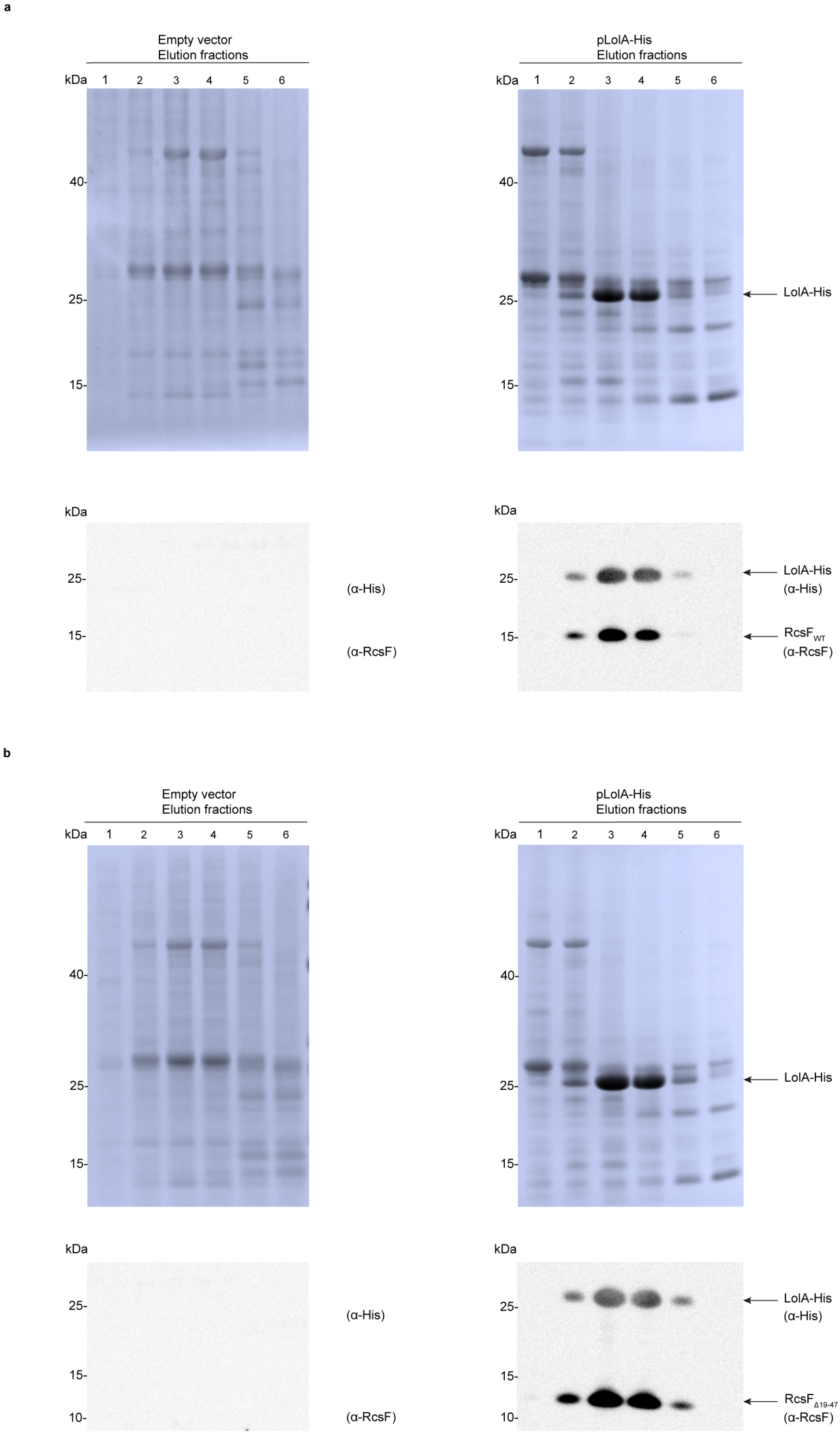
a
Empty vector
Elution fractions
pLolA-His
Elution fractions
kDa
1
2
3
4
5
6
40-
25-
15-
LolA-His
(α-His)
(α-RcsF)
RcsF$_{WT}$
b
10-
RcsF$_{\Delta 19-47}$

a

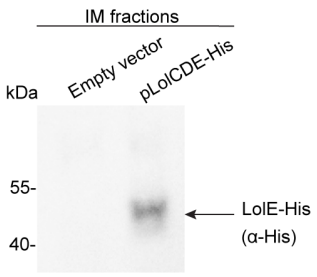
IM fractions
Empty vector
pLolCDE-His
kDa
55-
40-
LolE-His
(α-His)

b

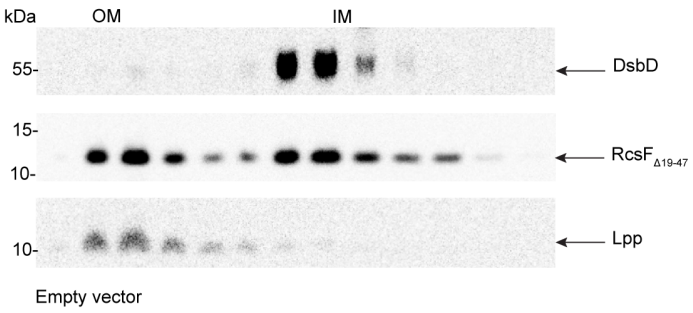
kDa
OM
IM
55-
DsbD
15-
10-
RcsF$_{\Delta 19-47}$
10-
Lpp
Empty vector

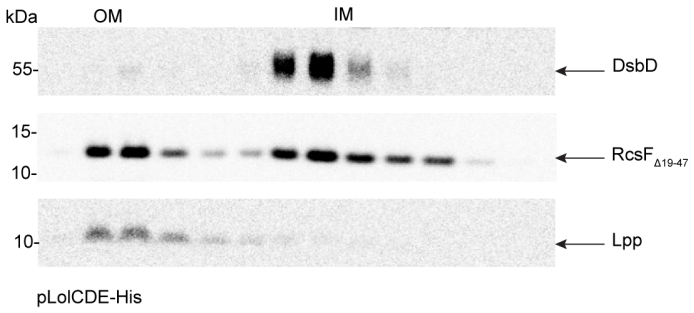
kDa
OM
IM
55-
DsbD
15-
10-
RcsF$_{\Delta 19-47}$
10-
Lpp
pLolCDE-His

a

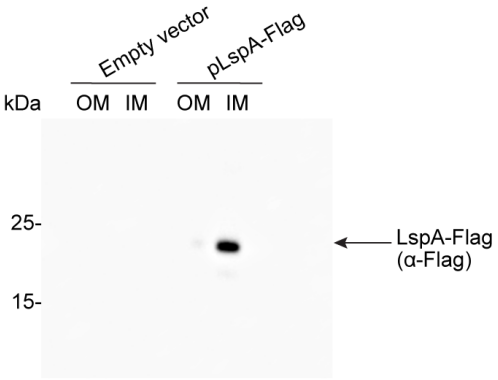
Empty vector
pLspA-Flag
kDa
OM IM OM IM
25-
15-
LspA-Flag
(α-Flag)

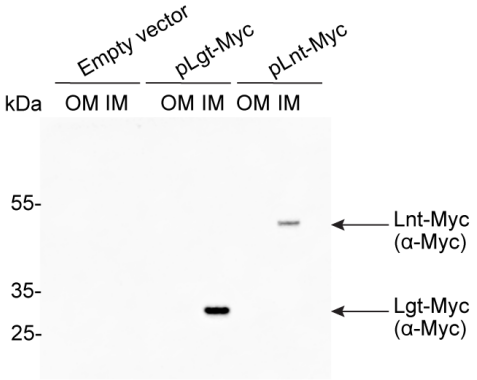
Empty vector
pLgt-Myc
pLnt-Myc
kDa
OM IM OM IM OM IM
55-
35-
25-
Lnt-Myc
(α-Myc)
Lgt-Myc
(α-Myc)

b

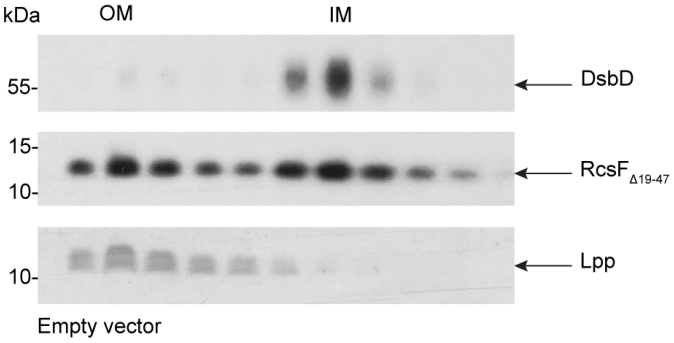
kDa
OM
IM
55-
15-
10-
10-
DsbD
RcsF Δ19-47
Lpp
Empty vector

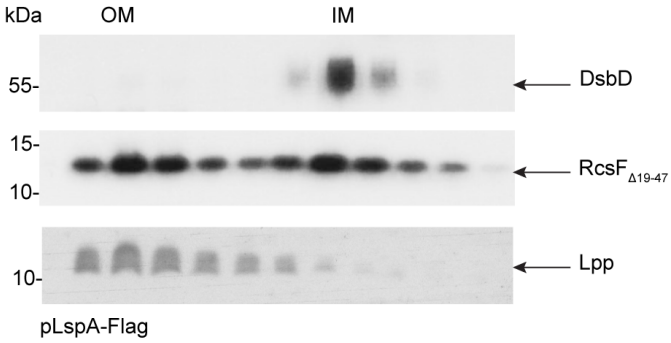
kDa
OM
IM
55-
15-
10-
10-
DsbD
RcsF Δ19-47
Lpp
pLspA-Flag

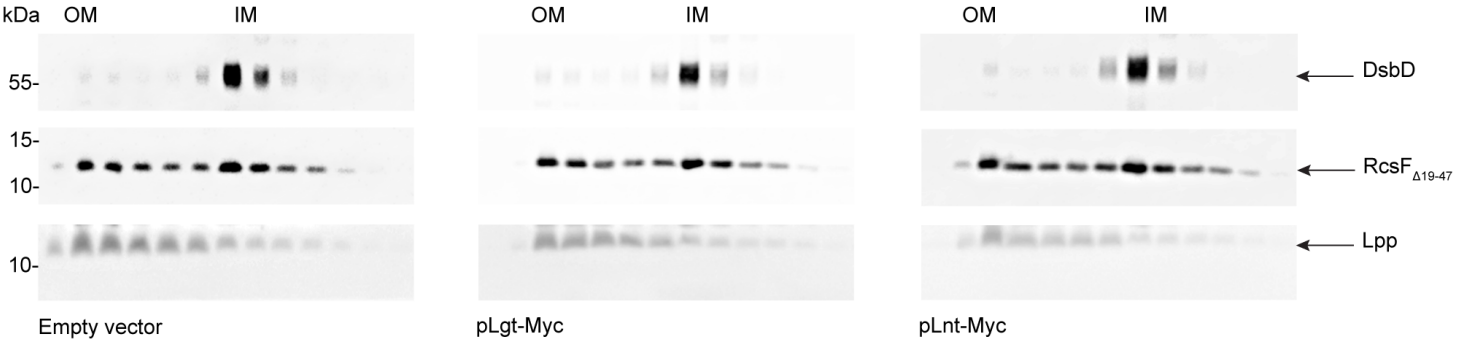
kDa
OM
IM
OM
IM
OM
IM
55-
15-
10-
10-
DsbD
RcsF Δ19-47
Lpp
Empty vector
pLgt-Myc
pLnt-Myc

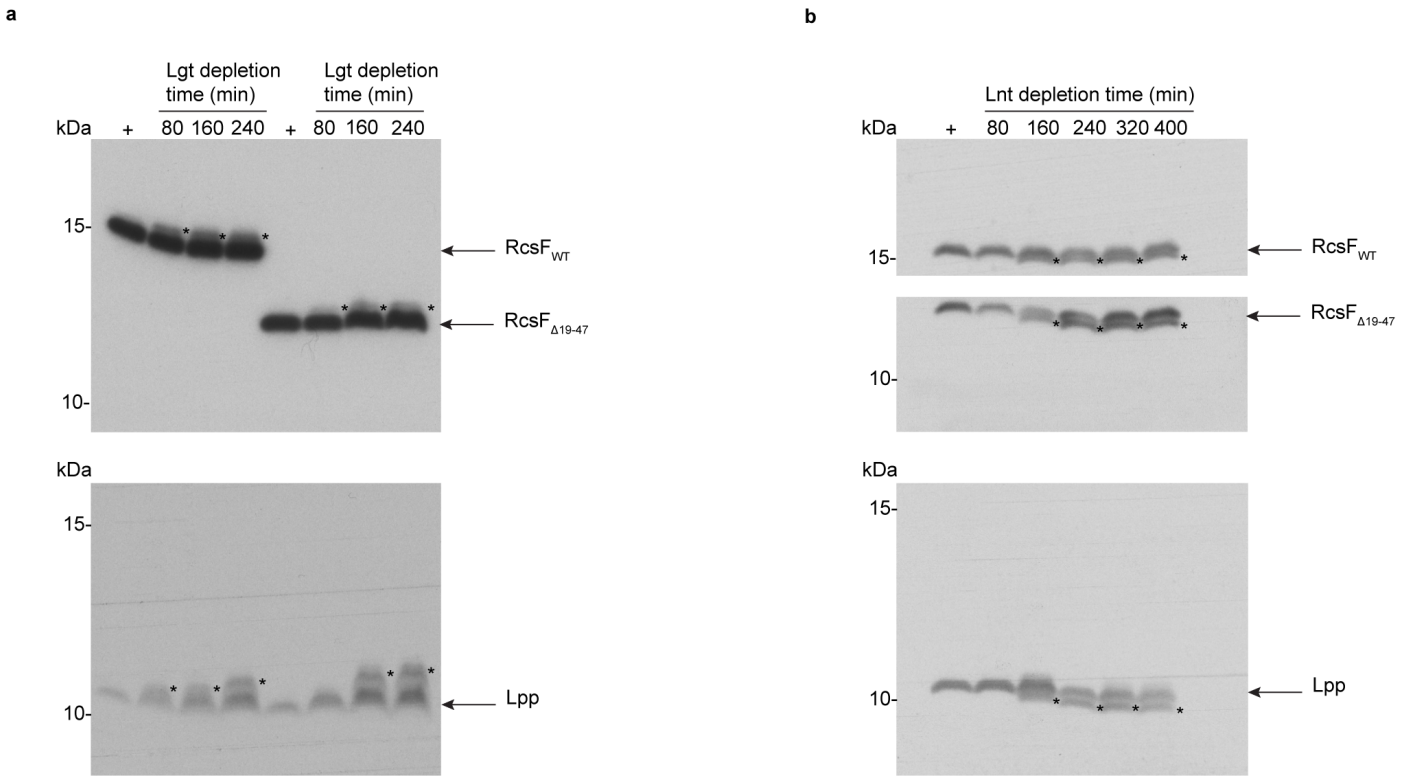
a
Lgt depletion time (min)
Lgt depletion time (min)
kDa + 80 160 240 + 80 160 240
15-
10-
RcsF$_{WT}$
RcsF$_{\Delta 19-47}$
kDa
15-
10-
Lpp
b
Lnt depletion time (min)
kDa + 80 160 240 320 400
15-
10-
RcsF$_{WT}$
RcsF$_{\Delta 19-47}$
kDa
15-
10-
Lpp

a

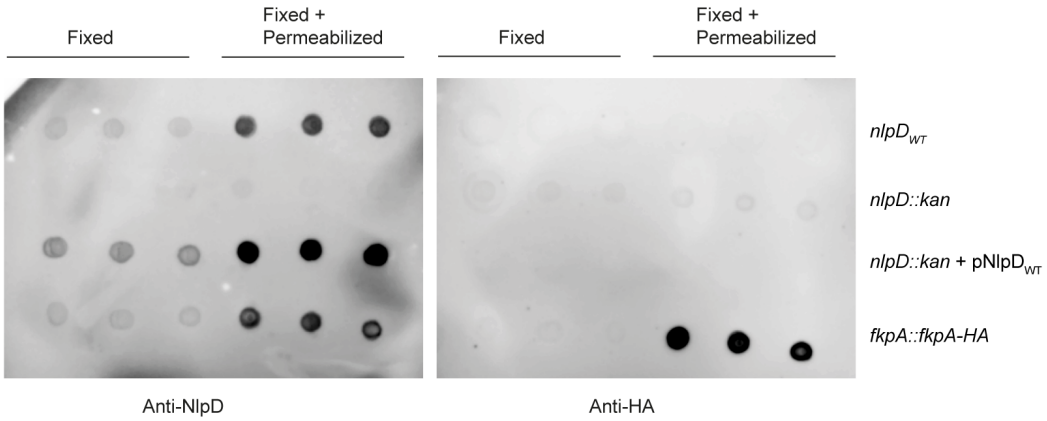
Fixed
Fixed + Permeabilized
Fixed
Fixed + Permeabilized
nlpD_WT
nlpD::kan
nlpD::kan + pNlpD_WT
fkpA::fkpA-HA
Anti-NlpD
Anti-HA

b

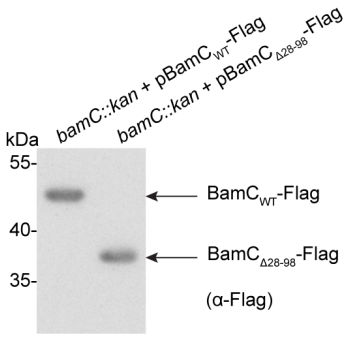
bamC::kan + pBamC_WT-Flag
bamC::kan + pBamC Δ28-98-Flag
kDa
55-
40-
35-
BamC_WT-Flag
BamC_Δ28-98-Flag
(α-Flag)

c

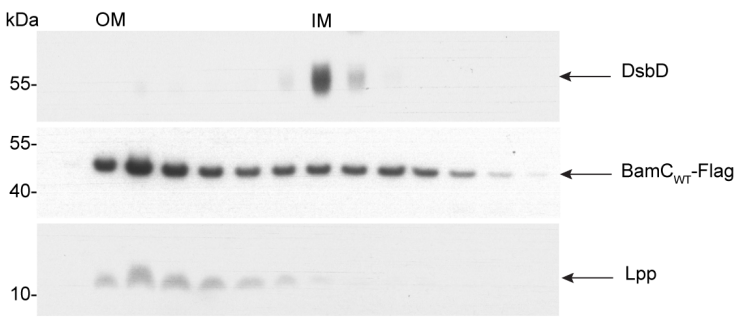
kDa
OM
IM
55-
55-
40-
10-
DsbD
BamC_WT-Flag
Lpp

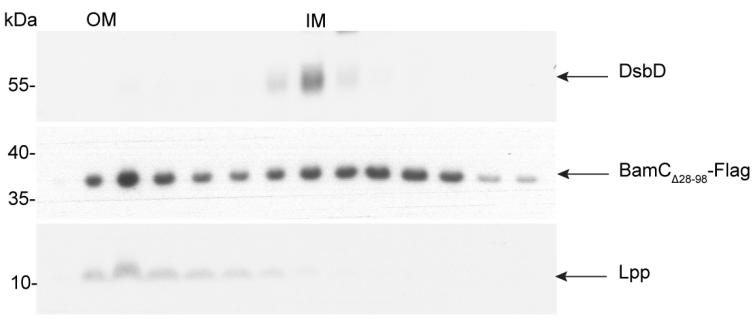
kDa
OM
IM
55-
40-
35-
10-
DsbD
BamC_Δ28-98-Flag
Lpp